British Journal of Cancer http://www.nature.com/bjc/

DOI : 10.1038/s41416-020-0744-7

Nintedanib inhibits intrahepatic cholangiocarcinoma aggressiveness via suppression of cytokines extracted from activated cancer-associated fibroblasts

Running title: Nintedanib for intrahepatic cholangiocarcinoma

Takahiro Yamanaka[1], Norifumi Harimoto[1], Takehiko Yokobori[2], Ryo Muranushi[1], Kouki Hoshino[1], Kei Hagiwara[1], Dolgormaa Gantumur[1], Tadashi Handa[3,4], Norihiro Ishii[1], Mariko Tsukagoshi[1,5], Takamichi Igarashi[1], Hiroshi Tanaka[1], Akira Watanabe[1], Norio Kubo[1], Kenichiro Araki[1], and Ken Shirabe[1]

[1] Department of General Surgical Science, Division of Hepatobiliary and Pancreatic Surgery, Gunma University, Graduate School of Medicine, Gunma, Japan

[2] Gunma University Initiative for Advanced Research (GIAR), Gunma, Japan

[3] Department of Diagnostic Pathology, Gunma University, Graduate School of Medicine, Gunma, Japan

[4]Department of Social Welfare, Gunma University of Health and Welfare, Gunma, Japan

[5] Department of Innovative Cancer Immunotherapy, Gunma University, Graduate School of Medicine, Gunma, Japan

Corresponding author: Norifumi Harimoto MD, PhD

Department of General Surgical Science, Division of Hepatobiliary and Pancreatic Surgery, Gunma University, Graduate School of Medicine, 3-39-22 Showamachi, Maebashi 371-8511, Gunma, Japan

Tel: +81-027-220-8224 Fax: +81-027-220-8230

E-mail: nharimotoh1@gunma-u.ac.jp

Abstract

Background: Intrahepatic cholangiocarcinoma (ICC) is a malignancy that is challenging to treat. Fibroblasts in ICC tissues have been identified as cancer-associated fibroblasts (CAFs) that promote the malignant behavior of ICC cells. An antifibrotic drug nintedanib has been reported to suppress activated hepatic stellate cells in liver fibrosis.

Methods: We investigated whether nintedanib could suppress the cancer-promoting effect of CAFs derived from ICC tissues *in vitro* and *in vivo*.

Results: CAFs promoted the proliferation and invasion of ICC cells. Nintedanib suppressed activated CAFs expressing α-smooth muscle actin (α-SMA) and inhibited the ICC promoting effects of CAFs. Nintedanib greatly reduced the levels of cancer-promoting cytokines, such as interleukin (IL)-6 (IL-6) and IL-8, secreted by CAFs. *In vivo* study demonstrated that nintedanib reduced xenografted ICC growth and activated CAFs expressing α-SMA and that combination therapy with nintedanib and gemcitabine against CAFs and ICC cells showed the strongest inhibition of tumor growth compared with the control and single treatment groups.

Conclusions: Nintedanib inhibited the cancer-promoting effect of CAFs via the suppression of CAF activation and secretion of cancer-promoting cytokines. Our findings suggest that therapeutic strategies combining conventional cytotoxic agents with nintedanib targeting CAFs is promising for overcoming refractory ICC with activated CAFs.

Background

Intrahepatic cholangiocarcinoma (ICC) is the second most common hepatic carcinoma, and its incidence has increased in recent years.[1,2] Despite recent advances in surgical techniques and chemotherapy, the prognosis of ICC remains poor.[3,4,5,6] Therefore, novel therapeutic strategies are required for improving the prognosis of ICC.

Compared with hepatocellular carcinoma (HCC), ICC presents with extensive fibrosis in the tumor.[7] Tumor fibrosis is caused by cancer-associated fibroblasts (CAFs), which are reported to play a key role in the ICC microenvironment and promote malignant behavior such as proliferation, invasion, metastasis, and resistance to therapy via interactive signaling pathways.[8,9,10,11] Indeed, some researchers have reported that CAF-secreted cytokines, such as interleukin (IL)-6 (IL-6), IL-8, C-C motif chemokine ligand 2 (CCL2), and C-X-C motif chemokine ligand 12 (CXCL12), can increase the aggressiveness of co-cultured cancer cells.[12,13,14] Moreover, a high expression of α-smooth muscle actin (α-SMA), a marker of activated CAFs, has been correlated with shorter survival times in patients who underwent surgical resection of ICC.[9,10] These findings suggest that targeting CAFs could be a novel strategy for controlling ICC aggressiveness caused by activated CAFs.

The FDA-approved antifibrotic drug nintedanib is a small molecule inhibitor of

multiple tyrosine kinases, such as fibroblast growth factor receptor (FGFR), vascular endothelial growth factor receptor (VEGFR), and platelet-derived growth factor receptor (PDGFR),[15] and reportedly, it is therapeutically effective in idiopathic pulmonary fibrosis.[16,17,18] It was previously reported that nintedanib evidently suppressed chemical-induced liver fibrosis via the suppression of activated hepatic stellate cells expressing α-SMA, which is a marker of activated-stellate cells.[19] Moreover, nintedanib was able to suppress the activation of CAFs expressing α-SMA in lung adenocarcinoma.[20] Therefore, we hypothesized that nintedanib treatment can inhibit the activation of CAFs expressing α-SMA in ICC. However, to the best of our knowledge, studies investigating the effects of nintedanib on CAFs derived from ICC tissues have not yet been conducted.

The aim of the present study was to clarify whether nintedanib could inhibit CAFs derived from ICC tissues. Therefore, we investigated the effects of nintedanib on ICC-derived CAFs that promoted the malignant behavior of ICC cells, such as proliferation and invasion. In addition, using an *in vivo* xenograft model co-implanted with CAFs and ICC cells, we assessed the therapeutic efficacy of combining conventional cytotoxic agents, such as gemcitabine, with nintedanib to target the activated CAFs.

Materials and Methods

Cell cultures and cell isolation

We established primary CAFs (CAF1 and CAF2) from surgically resected ICC tissues in Gunma University, using the method described by Lau et al.[21] Briefly, ICC tissues were minced into small pieces and incubated in Dulbecco's modified Eagle medium (DMEM, Wako, Osaka, Japan) supplemented with 20% fetal bovine serum (FBS), 1% penicillin–streptomycin (Thermo Fisher Scientific, Kanagawa, Japan), and 1 ng/mL basic fibroblast growth factor (bFGF, Wako) and were maintained at 37 °C in a humidified incubator with 5% CO_2 to allow attachment to the culture plate. We then removed the unattached cells and replenished the medium repeatedly twice a week. We confirmed that the CAFs exhibited a myofibroblast-like morphology; moreover, the positive expression of α-SMA was confirmed using Western blotting. For our experiments, we used the CAFs between passage numbers 4 and 8. The establishment of CAFs from surgically resected ICC tissues was approved by the Institutional Review Board of Gunma University (Approval number: 2016-118). The human ICC cell lines, HuCCT1 and RBE, were used in the present study. The HuCCT1 cell line was provided by RIKEN BRC (Bio-Resource Center) in Japan and authenticated by short tandem

repeat DNA profiling by BEX Co., Ltd. (Tokyo, Japan). The RBE cell line was also provided by RIKEN BRC. Cells were cultured in DMEM supplemented with 10% FBS and 1% penicillin–streptomycin (Thermo Fisher Scientific, Kanagawa, Japan) and maintained at 37°C in a humidified incubator with 5% CO_2 atmosphere.

Nintedanib (BIBF1120)

The nintedanib used in the present study was purchased from Selleck (TX, USA) and Med Chem Express (NJ, USA). Briefly, nintedanib was dissolved in dimethyl sulfoxide (DMSO, Wako, Osaka, Japan) at a final concentration of 1-10 nM/mL for the *in vitro* experiments. Nintedanib was dissolved in Tween-80 (Sigma-Aldrich) solution at a final concentration of 30mg/kg for the *in vivo* experiments.

Protein extraction and Western blotting

CAFs were treated with nintedanib at concentrations varying between 0 and 3 μM and 5ng/mL recombinant transforming factor β (TGFβ, R＆D systems, Minneapolis, USA) for 72 hours followed by protein extraction. ICC cell lines were treated with nintedanib, CAF-conditioned medium (CM), and nintedanib-treated CAF-CM for 12 hours, followed by protein extraction. Cells of the ICC cell line were treated with 10 ng/ml

recombinant IL-6 Protein (R&D systems) and 10 ng/ml recombinant IL-8 Protein (R&D systems) for 2 hours, followed by protein extraction. Protein extraction was performed using RIPA buffer (Wako) containing phosphatase inhibitor (p2850; Sigma-Aldrich) according to the manufacturer's instructions. Proteins were separated using SDS–PAGE with 10% Bis–Tris gels and transferred to nitrocellulose membranes (#12369; Cell signaling). Membranes were blocked with 5% skimmed milk or 5% BSA and incubated overnight at 4°C with the primary antibodies. The primary antibodies used in the present study were anti-α-SMA mouse monoclonal antibody (A2547; 1:1000; Sigma-Aldrich, St. Louis, MO, USA), Phospho-STAT3 rabbit antibody (#9145; 1:1000; Cell Signaling Technology, MA, USA), STAT3 mouse antibody (#9139S; 1:1000; Cell Signaling Technology), and anti-β-actin mouse monoclonal antibody (A5316; 1:1000; Sigma-Aldrich) as a loading control. Next, membranes were treated with horseradish peroxidase (HRP)-conjugated secondary antibodies. Protein bands on the membrane were detected using ECL™ Prime Western Blotting Detection Reagent and an ImageQuant™ LAS 4000 imager (GE Healthcare, Buckinghamshire, UK).

Conditioned medium

CAFs were cultured in DMEM supplemented with 20% FBS and 1ng/mL bFGF until

they reached a confluence of 90%. Next, the medium was changed to serum-free DMEM and the cells were cultured for an additional 120 h. At the end of the incubation, CAF-CM was collected and centrifuged for 10 min at 1500 g. In order to evaluate the effect of nintedanib, CAFs were cultured in serum-free DMEM containing 1μM nintedanib for 120 h and collected as nintedanib-treated CAF-CM.

Ultracentrifugation

Ultracentrifugation was performed as previously described[13]. Briefly, CAF-CM was ultracentrifuged at 110,000× *g* for 70 min at 4°C. The supernatant was collected after the first centrifugation. The pellets were washed with phosphate-buffered saline, subjected to ultracentrifugation, and resuspended in serum-free DMEM.

Cell proliferation assay

The cell proliferation assay was performed using a Cell Counting Kit-8 (CCK-8; Dojindo Laboratories, Kumamoto, Japan). The CAFs and ICC cell lines were seeded in 96-well plates and cultured. Culture medium was changed to serum-free medium containing nintedanib at concentrations varying between 0 and 10 μM. To assess cell proliferation after stimulation with CM, the medium of ICC cells was also replaced with

CAF-CM or nintedanib-treated CAF-CM after overnight incubation. Cell proliferation was evaluated after 48 h. The absorbance of each well was measured using a spectrophotometer (Bio-Rad, Hercules, CA, USA) at 450 nm with the reference wavelength set at 650 nm.

Invasion assay

The cell invasion assay was performed using 24-well Corning® BioCoat™ Matrigel Invasion Chambers (Corning, NY, USA). ICC cell lines were seeded in the upper chamber in FBS-free medium, and the lower chamber was filled with medium supplemented with 3% FBS and containing 1 μM nintedanib, CAF-CM, or nintedanib-treated CAF-CM. After incubation for 48 h, the cells were fixed and stained with Diff-Quik (Sysmex Corporation, Kobe, Japan). After staining, cells that migrated through the pores to the lower surface of the membrane were counted under the microscope. In total, 5 randomly selected fields were evaluated.

Cytokine array and enzyme-linked immunosorbent assay (ELISA)

Cytokine profiles of cells treated with CAF-CM and nintedanib-treated CAF-CM were compared using the Proteome Profiler Human XL Cytokine Array Kit (ARY022B; R&D

Systems, MN, USA), according to the manufacturer's instructions. Detection and quantification of the array spots were performed using the ImageQuant™ LAS 4000 imager (GE Healthcare). Concentrations of cytokines in CAF-CM and nintedanib-treated CAF-CM treated cells were measured using the enzyme-linked immunosorbent assay (ELISA). The IL-6 (ab46027) and IL-8 (ab46032) ELISA kits were purchased from Abcam (Cambridge, MA, USA) and used according to the manufacturer's instructions.

In vivo experiments

First, to investigate the effect of CAFs in an *in vivo* xenograft model, we compared the proliferation rates of HuCCT1 cells alone and HuCCT1 plus CAFs cells. HuCCT1 cell suspensions (5×10^6 cells) and HuCCT1 (5×10^6 cells) plus CAF (1×10^6 cells) cell suspensions were bilateral subcutaneously injected into the flanks of isoflurane-anesthetized 7-week-old female NOD-SCID mice (CLEA Japan, Inc., Tokyo, Japan). Each group contained 5 xenografts. The experiment was conducted as per the schedule given in Supplementary Figure 1A. Moreover, to analyze the effects of nintedanib *in vivo*, we used a mouse xenograft model of HuCCT1 plus CAFs cells. Two weeks after implantation, we randomly divided mice into the control, nintedanib,

gemcitabine, and nintedanib and gemcitabine groups. We administered 30mg/kg nintedanib orally five times a week and 50 mg/kg gemcitabine intraperitoneally twice a week to mice under isofurane anesthesia. Each group contained 6 xenografts. The experiment was conducted as per the schedule given in Supplementary Figure 1B.Tumor diameters and body weights were measured twice a week and tumor volume was calculated using the following formula: S × S × L/2, where S is the short diameter of the tumor, and L is the long diameter of the tumor. To collect xenografted tumors, mice were anesthetized with isoflurane and euthanised via cervical dislocation. The tumors were microscopically evaluated using hematoxylin and eosin staining and immunohistochemistry. To evaluate adverse events of treatment, we obtained blood samples from mice; serum biochemical tests were conducted by the Oriental Yeast Co. (Tokyo, Japan). Mice had free access to water and food and were housed in specific pathogen-free cages and bedding in a 12-h light/dark regimen with controlled room temperature. All mouse experiments were performed in compliance with the guidelines of the Institute for Laboratory Animal Research at Gunma University, Maebashi, Japan (Approval number: 18-024).

Immunohistochemistry

Immunohistochemistry analysis of tumor samples was performed using the following primary antibodies: mouse monoclonal anti-α-SMA antibody (A5247; 1:1000; Sigma-Aldrich), anti-Ki-67 antibody (M7240; 1:200; Dako; Agilent Technologies, CA, USA), and phospho-STAT3 rabbit antibody (#9145; 1:200; Cell Signaling Technology). The amount of α-SMA and Ki-67 positive cells were measured using the ImageJ 1.51 image analysis software (National Institute of Health, MD, USA). The number of phospho-STAT3-positive cells was counted under the microscope.

Statistical analysis

Data for continuous variables are expressed as means ± standard deviation (SD). Differences between two groups were estimated using *t*-tests. Differences among four groups were evaluated using ANOVA with Tukey's multiple comparison tests. All $p < 0.01$ or 0.05 were considered statistically significant. All statistical analyses were performed using the statistics software Easy R (EZR).

Results

ICC-derived-CAFs promote proliferation and invasion of ICC cells *in vitro*

In order to confirm the effect of CAFs on cancer progression, we evaluated the cancer

proliferation and invasion of ICC cell lines treated with CAF-CM. CAF-CM promoted the proliferation and invasion of ICC cell lines (Figure 1A, and Figure 1B). Moreover, the tumor volume of HuCCT1 cells co-implanted with CAFs grew to a size larger than those of HuCCT1 cells alone *in vivo* (Figure 1C).

Antifibrotic drug nintedanib suppresses the activation of CAFs

In order to examine the effect of nintedanib on CAFs and ICC cell lines, we evaluated the effect of nintedanib on the proliferation of CAFs and ICC cell lines. Nintedanib significantly suppressed CAF proliferation in a concentration-dependent manner compared with the control (Figure 2A). On the other hand, the suppression effect of nintedanib against ICC cell lines was observed only at the high concentrations of 3 or 10 μM (Figure 2B). Moreover, nintedanib suppressed the expression of α-SMA, an activated CAF marker, in CAF1 and CAF2 cells in a concentration-dependent manner, (Figure 2C).

Nintedanib could eliminate the CAF induced proliferative and invasive abilities of ICC cells

In order to determine the effects of nintedanib on the malignant behavior of ICC cell

lines induced by CAFs, we investigated the proliferative and invasive capabilities of the ICC cell lines using nintedanib-treated CAF-CMs. As mentioned above, there was no significant direct effect of a low (1μM) nintedanib concentration on the proliferation and invasion of ICC cell lines (Figure 3A and Figure 3B), and the CAF-CM increased the proliferation and invasion of ICC cells. Interestingly, the proliferation-enhancing effects of CAF-CM were eliminated by nintedanib treatment (Figure 3A), and it was observed that nintedanib could decrease CAF-CM enhanced ICC cell line invasion (Figure 3B).

Nintedanib suppressed cytokine secretion by CAFs

To determine the factors involved in CAF suppression by nintedanib, we used ultracentrifugation to allow the evaluation of soluble factors such as cytokines, and the pellet after ultracentrifugation, which might include the extracellular vesicles. The supernatants of CAF-CM after ultracentrifugation promoted the proliferation of cancer cells. This effect was eliminated by treatment with nintedanib, as with the original solutions. Conversely, the resuspended pellets did not exhibit any significant effect on the cancer cells (Supplementary Figure 2). Subsequently, we performed cytokine array analysis to evaluate the differences between control CAF-CM and CAF-CM treated

with nintedanib for 105 types of soluble factors, including cytokines and proteins (Supplementary Table 1). Although various cytokines and proteins were suppressed by nintedanib treatment, interleukin-6 (IL-6), interleukin-8 (IL-8), vascular endothelial growth factor (VEGF), vascular cell adhesion molecule 1 (VCAM1) and osteopontin were remarkably decreased in the nintedanib-treated CAF-CM compared with the control (Figure 4A). Among these, we focused on IL-6 and IL-8 as the cytokines that were significantly suppressed by nintedanib, and we validated the significant suppression of IL-6 and IL-8 in nintedanib-treated CAF-CM using ELISA (Figure 4B). Moreover, we confirmed the effects of CAF-CM and nintedanib-treated CAF-CM on the phosphorylation of STAT3, which is known as a representative downstream target of several external cytokines including IL-6 and IL-8. CAF-CM remarkably increased the phosphorylation of STAT3 in ICC cell lines, but the increasing effects on CAF phosphorylation were eliminated by nintedanib treatment (Figure 4C). We confirmed that treatment with recombinant IL-6 and IL-8 protein promoted the phosphorylation of STAT3 (Supplementary Figure 3A). Moreover, we confirmed that nintedanib-treated CAF-CM with recombinant IL-6 and IL-8 protein restored the cancer-promoting effects of CAFs (Supplementary Figure 3B).

Nintedanib inhibits tumor proliferation, and combination therapy with gemcitabine inhibits tumor proliferation even more remarkably

We investigated the combined effect *in vivo* of nintedanib and gemcitabine, which is a standard therapeutic drug against ICC in clinical practice. Although treatment with nintedanib alone and gemcitabine alone inhibited tumor proliferation, therapy with nintedanib and gemcitabine combined inhibited tumor growth to an even greater degree than with each agent. Additionally, tumor shrinkage, as compared with the tumor volume on day 0, was only observed in the nintedanib and gemcitabine combination therapy group (Figure 5A). The tumors treated with nintedanib showed a reduction of α-SMA-positive staining area compared with controls or those treated with gemcitabine alone (Figure 5B). The proportion of Ki-67 positive ICC cells was significantly lower in tumors treated with gemcitabine compared with controls or those treated with nintedanib (Figure 5B). Tumors treated with nintedanib and gemcitabine combined showed a reduction of both the α-SMA-positive staining area and the proportion of Ki-67 positive ICC cells (Figure 5B). Nintedanib treatment resulted in a significant reduction in the number of pSTAT3-positive cells, with the greatest reduction observed with combined nintedanib and gemcitabine treatment (Supplementary Figure 4). Although we evaluated adverse events associated with the treatments *in vivo*, there were

no significant differences among the groups regarding body weight and organ toxicity (Supplementary Figure 5A, 5B).

Discussion

Herein, we have demonstrated that CAFs promoted ICC malignancy *in vitro* and *in vivo*, and nintedanib treatment suppressed the ability of CAFs to enhance the aggressiveness of ICC cells. This study is the first report to show the CAF suppression effect of nintedanib *in vivo*. We also showed that various cytokines produced by CAFs, such as IL-6, IL-8, VEGF, VCAM1, and osteopontin, were strongly suppressed by the treatment with the antifibrotic drug nintedanib. Moreover, *in vivo* experiments showed that nintedanib suppressed the α-SMA-positive staining area in tumors and that combination therapy with gemcitabine inhibited tumor growth to an even greater extent compared with single-agent treatment. It was suggested that targeting strategy against both CAFs by nintedanib and ICC cells by gemcitabine is a useful therapeutic tool to treat refractory ICC with activated CAFs.

Recently, tumor-stromal interactions in cancer tissues have been recognized as playing important roles in tumor progression, and have been highlighted in several reviews.[9,10,11] To target the tumor-stromal interactions, anticancer therapy against not

only cancer cells but also stromal CAFs has actively been investigated. Recent studies have shown that navitoclax,[22] resveratrol,[12] and everolimus[23] suppressed CAFs in cholangiocarcinomas. Previously, we reported that the antifibrotic drug conophylline, a natural vinca alkaloid compound, could inhibit pancreatic cancer progression through the suppression of CAFs originated from stellate cells in pancreatic cancer.[13] Consistent with our previous findings, some researchers reported the fundamental effect of conophylline as an inhibitor of activated-stellate cells in the liver and pancreas.[24,25] In this study, we focused on the effect of the FDA-approved, antifibrotic drug nintedanib against CAFs derived from ICC tissues. Nintedanib is an inhibitor of multiple tyrosine kinases, such as FGFR, VEGFR, and PDGFR, and it has shown therapeutic effects against stromal fibrosis in patients with idiopathic pulmonary fibrosis.[16,17,18] It was previously reported that nintedanib clearly suppressed chemical-induced liver fibrosis through the suppression of activated hepatic stellate cells with α-SMA, which is a marker of activated-stellate cells.[19] In this study, antifibrotic drug nintedanib suppressed activated CAFs with α-SMA which could enhance the aggressiveness of ICC cells. From these observations, antifibrotic drugs such as nintedanib may be candidates for the inhibition of tumor-stromal interaction, including cancer cells and CAFs via suppression of activated CAFs with α-SMA.

Nintedanib has been shown to inhibit the proliferation and activation of lung fibroblasts and hepatic stellate cells.[18,19] Moreover, nintedanib has been shown to inhibit the tumor-promoting effect of CAFs in lung adenocarcinoma using CAF-CMs *in vitro*.[20] The activation of PDGF/PDGFR and FGF/FGFR signaling has been reported to significantly induce the proliferation and activation of fibroblasts including CAFs[26,27,28]; however, as mentioned above, nintedanib has been known to inhibit PDGFR and FGFR.[15] Moreover, it was reported that cholangiocarcinoma cells stimulated migration of CAFs via PDGF secretion.[29] In the present study, we showed that nintedanib suppressed the proliferation and activation of CAFs of ICC *in vitro* and *in vivo*. Therefore, it was suggested that nintedanib inhibits the activation of CAFs derived from ICC via suppression of CAFs activators such as PDGF/PDGFR and FGF/FGFR signaling pathways.

In a clinical trial aimed to clarify the anti-tumor effect of nintedanib monotherapy for patients with colorectal cancer, the monotherapy could not improve the overall survival of these patients.[30] Conversely, nintedanib, in combination with docetaxel, has been used for the second-line treatment in patients with advanced non-small cell lung cancer.[31] In the present study, a low concentration (1μM) of nintedanib could not suppress the proliferation of ICC cell lines (Figure 2). Nintedanib

was suggested to be more effective on CAFs than cancer cells because the low concentration (1μM) of nintedanib could specifically suppress the CAF activation and secretion of cytokines *in vitro*. In an *in vivo* study, administration of nintedanib alone could strongly suppress the stromal α-SMA-positive staining of xenograft tumors but could not suppress the proportion of Ki-67 positive ICC cells as strongly. The results of our study also suggested that nintedanib specifically suppresses the proliferation and activation of CAFs *in vivo*. Conversely, administration of gemcitabine alone could suppress the proportion of Ki-67 positive ICC cells in a xenograft tumor but could not suppress the stromal α-SMA-positive staining. Gemcitabine, a representative cytotoxic agent that acts on proliferating cancer cells, was suggested to be effective only on ICC cells with high proliferation potency. Interestingly, the combination treatment with nintedanib and gemcitabine showed tumor shrinkage as well as reduction of stromal α-SMA-positive staining and Ki-67 positive ICC cells. These data suggested that nintedanib and gemcitabine suppressed both activated CAFs with α-SMA and proliferating ICC cells, respectively. Therefore, combination therapy with nintedanib and cytotoxic agents, such as gemcitabine and docetaxel, may be very effective against cancers with activated CAFs with α-SMA.

In the present study, we showed that nintedanib suppressed the activation of

CAFs and significantly inhibited the secretion of various cytokines, especially IL-6, IL-8, VEGF, VCAM1, and osteopontin. These factors have been reported to play important roles in tumor growth. For instance, IL-6 was reported to regulate JAK-STAT3 signaling which promotes the proliferation of tumor cells, invasion, and immunosuppression.[32,33,34,35] IL-8 was reported to promote the proliferation of tumor cells, invasion, and metastasis in lung cancer and pancreatic cancer. [14, 36,37] VCAM1 is involved in the micro-environmental interaction between tumor cells and stromal cells and promotes the metastasis of breast cancer cells.[38] VEGF was reported to promote cancer proliferation and angiogenesis.[39,40] Osteopontin was reported to be a prognostic marker of ICC and promote the metastasis of ICC.[41,42] From the above-mentioned findings, the nintedanib might suppress the ICC promoting effects of CAFs through suppression of these cytokines.

In this study, we showed that nintedanib could suppress cancer-related cytokines, particularly, IL-6, IL-8, and VEGF. IL-6 was reported to induce the chemoresistance in cancer via activation of STAT3.[43] IL-8 and VEGF were reported to activate STAT3 in cancer cells.[44,45] The activation of STAT3 seems to be important for chemoresistance in cholangiocarcinoma cells.[46] Moreover, activated STAT3 was reported to induce resistance to gemcitabine in pancreatic cancer.[47,48] In this study, we

showed that the nintedanib not only suppressed the secretion of the cancer-promoting cytokines induced by CAFs but also the phosphorylation of STAT3 in ICC cells, which is induced by CAFs. Therefore, our results suggest that the combination of nintedanib and gemcitabine can promote the regulation of CAF-secreting cytokines which can cause gemcitabine resistance via activation of STAT3 in ICC cells.

Our study had some limitations. First, we did not perform sorting to collect the a pure CAF population using flow cytometric analysis. Therefore, there is a potential limitation of contamination with mesenchymal cells. Second, previous studies have reported that nintedanib can suppress not only CAFs but also non-cancer derived fibroblastic cells. We confirmed that nintedanib could suppress proliferation and α-SMA expression of non-cancer-derived fibroblasts LX-2 (hepatic stellate cell line) (Supplementary Figure 6). Therefore, we cannot exclude the possibility of off-target effects against non-cancer-derived fibroblasts in the whole body in the *in vivo* experiment.

In conclusion, we demonstrated that nintedanib inhibited the cancer-promoting effect of CAFs via suppression of CAF activation and secretion of multiple cancer-promoting cytokines. Nintedanib may be a useful tool to simultaneously regulate the activated CAFs and cancer-promoting cytokines. Moreover, we showed that the

combination of gemcitabine and nintedanib, one targeting cancer cells and the other targeting CAFs, respectively significantly reduced the tumor volume in xenografted tumor models. Therefore, combination therapy with nintedanib and cytotoxic agents may be a promising therapy to overcome refractory ICC with activated CAFs.

Additional Information

Ethics approval and consent to participate

The establishment of CAFs from surgically resected ICC tissues was approved by the Institutional Review Board of Gunma University (Approval number: 2016-118). Consent to participate was obtained from the patients. All mouse experiments were performed in compliance with the guidelines of the Institute for Laboratory Animal Research at Gunma University, Maebashi, Japan (Approval number: 18-024). Our study was performed in accordance with the Declaration of Helsinki.

Consent for publication

None

Data availability

All data generated or analyzed during this study are included in this article.

Conflict of interest

The authors declare no conflicts of interest.

Funding

The present study was supported by Grants-in-Aid for Scientific Research from the Japan Society for the Promotion of Science (grant numbers JP18H02877).

Authors' contributions

TY designed the study and wrote the initial draft of the manuscript. NH, TY, and KS contributed to analysis and data interpretation and assisted in the preparation of the manuscript. All other authors have contributed to data collection and interpretation and have critically reviewed the manuscript. All authors have approved the final version of the manuscript and agree to be accountable for all aspects of the work.

Acknowledgements

The authors would like to thank Enago (www.enago.com) for the English language review.

Supplementary information is available at the British Journal of Cancer's website

References

1. Everhart JE, Ruhl CE. Burden of digestive diseases in the United States Part III, Liver, biliary tract, and pancreas. *Gastroenterology* 2009, **136**(4), 1134–1144

2. Khan SA, Taylor-Robinson SD, Toledano MB, Beck A, Elliott P, Thomas HC. Changing international trends in mortality rates for liver, biliary and pancreatic tumours. *J Hepatol* 2002, **37**(6), 806–813

3. Aljiffry M, Abdulelah A, Walsh M, Peltekian K, Alwayn I, Molinari M. Evidence-based approach to cholangiocarcinoma, a systematic review of the current literature. *J Am Coll Surg* 2009, **208**(1), 134–147

4. DeOliveira ML, Cunningham SC, Cameron JL, Kamangar F, Winter JM, Lillemoe KD, et al, Cholangiocarcinoma, thirty-one-year experience with 564 patients at a single institution. *Ann Surg* 2007, **245**(5), 755–762

5. Gores GJ. Cholangiocarcinoma, current concepts and insights. *Hepatology* 2003, **37**(5), 961–969

6. Patel T. Cholangiocarcinoma--controversies and challenges. *Nat Rev Gastroenterol Hepatol* 2011, **8**(4), 189–200

7. Tadashi T, Kiyoko M, Noboru T, Yasuo S, Yasuni N. Alpha-smooth muscle actin-positive stromal cells in cholangiocarcinomas, hepatocellular carcinomas and metastatic liver carcinomas. *J Hepatol* 1996, **24**(6), 706–712

8. Kalluri R, Zeisberg M. Fibroblasts in cancer. *Nat Rev Cancer* 2006, **6**(5), 392–401

9. Okabe H, Beppu T, Hayashi H, Horino K, Masuda T, Komori H et al. Hepatic stellate cells may relate to progression of intrahepatic cholangiocarcinoma. *Ann Surg Oncol* 2009, **16**(9), 2555–2564

10. Chuaysri C, Thuwajit P, Paupairoj A, Chau-In S, Suthiphongchai T, Thuwajit C. Alpha-smooth muscle actin-positive fibroblasts promote biliary cell proliferation and correlate with poor survival in cholangiocarcinoma. *Oncol Rep* 2009, **21**(4), 957–969

11. Sirica AE. The role of cancer-associated myofibroblasts in intrahepatic cholangiocarcinoma. *Nat Rev Gastroenterol Hepatol* 2011, **9**(1), 44–54

12. Thongchot S, Ferraresi A, Vidoni C, Loilome W, Yongvanit P, Namwat N et al. Resveratrol interrupts the pro-invasive communication between cancer associated fibroblasts and cholangiocarcinoma cells. *Cancer Lett* 2018, **430**, 160–171

13. Ishii N, Araki K, Yokobori T, Hagiwara K, Gantumur D, Yamanaka T et al. Conophylline suppresses pancreatic cancer desmoplasia and cancer-promoting cytokines produced by cancer-associated fibroblasts. *Cancer Sci* 2019, **110**(1), 334–344

14. Wang T, Notta F, Navab R, Joseph J, Ibrahimov E, Xu J et al. Senescent Carcinoma-Associated Fibroblasts Upregulate IL8 to Enhance Prometastatic Phenotypes. *Mol Cancer Res* 2017, **15**(1), 3–14

15. Hilberg F, Roth GJ, Krssak M, Kautschitsch S, Sommergruber W,

Tontsch-Grunt U et al. BIBF 1120, triple angiokinase inhibitor with sustained receptor blockade and good antitumor efficacy. *Cancer Res* 2008, **68**(12), 4774–4782

16. Richeldi L, Costabel U, Selman M, Kim DS, Hansell DM, Nicholson AG et al. Efficacy of a tyrosine kinase inhibitor in idiopathic pulmonary fibrosis. *N Engl J Med* 2011, **365**(12), 1079–1087

17. Richeldi L, Du Bois RM, Raghu G, Azuma A, Brown KK, Costabel U et al. Efficacy and safety of nintedanib in idiopathic pulmonary fibrosis. *N Engl J Med* 2014, **370**(22), 2071–2082

18. Wollin L, Maillet I, Quesniaux V, Holweg A, Ryffel B. Antifibrotic and anti-inflammatory activity of the tyrosine kinase inhibitor nintedanib in experimental models of lung fibrosis. *J Pharmacol Exp Ther* 2014, **349**(2), 209–220

19. Akcora BÖ, Storm G, Prakash J, Bansal R. Tyrosine kinase inhibitor BIBF1120 ameliorates inflammation, angiogenesis and fibrosis in CCl4-induced liver fibrogenesis mouse model. *Sci Rep* 2017, **7**, 44545

20. Gabasa M, Ikemori R, Hilberg F, Reguart N, Alcaraz J. Nintedanib selectively inhibits the activation and tumour-promoting effects of fibroblasts from lung adenocarcinoma patients. *Br J Cancer* 2017, **117**(8), 1128–1138

21. Lau EY, Lo J, Cheng BY, Ma MK, Lee JM, Ng JK et al. Cancer-Associated

Fibroblasts Regulate Tumor-Initiating Cell Plasticity in Hepatocellular Carcinoma through c-Met/FRA1/HEY1 Signaling. *Cell Rep* 2016, **15**(6), 1175–1189

22. Mertens JC, Fingas CD, Christensen JD, Smoot RL, Bronk SF, Werneburg NW et al. Therapeutic effects of deleting cancer-associated fibroblasts in cholangiocarcinoma. *Cancer Res* 2013, **73**(2), 897–907

23. Heits N, Heinze T, Bernsmeier A, Kerber J, Hauser C, Becker T et al. Influence of mTOR-inhibitors and mycophenolic acid on human cholangiocellular carcinoma and cancer associated fibroblasts. *BMC Cancer* 2016, **16**, 322

24. Kubo N, Saito R, Hamano K, Nagasawa M, Aoki F, Takei I et al. Conophylline suppresses hepatic stellate cells and attenuates thioacetamide-induced liver fibrosis in rats. *Liver Int* 2014, **34**(7), 1057–1067

25. Saito R, Yamada S, Yamamoto Y, Kodera T, Hara A, Tanaka Y et al. Conophylline suppresses pancreatic stellate cells and improves islet fibrosis in Goto-Kakizaki rats. *Endocrinology* 2012, **153**(2), 621–630

26. Elenbaas B, Weinberg RA. Heterotypic signaling between epithelial tumor cells and fibroblasts in carcinoma formation. *Exp Cell Res* 2001, **264**(1), 169–184

27. Kuzet SE, Gaggioli C. Fibroblast activation in cancer, when seed fertilizes soil. *Cell Tissue Res* 2016, **365**(3), 607–619

28. MacKenzie B, Korfei M, Henneke I, Sibinska Z, Tian X, Hezel S et al. Increased FGF1-FGFRc expression in idiopathic pulmonary fibrosis. *Respir Res* 2015, **16**, 83

29. Cadamuro M, Nardo G, Indraccolo S, Dall'Olmo L, Sambado L, Moserle L et al. Platelet-derived growth factor-D and Rho GTPases regulate recruitment of cancer-associated fibroblasts in cholangiocarcinoma. *Hepatology* 2013, **58**(3), 1042–1053

30. Van Cutsem E, Yoshino T, Lenz HJ, Lonardi S, Falcone A, Limón ML et al. Nintedanib for the treatment of patients with refractory metastatic colorectal cancer (LUME-Colon 1), a phase III, international, randomized, placebo-controlled study. *Ann Oncol* 2018, **29**(9), 1955–1963

31. Popat S, Mellemgaard A, Fahrbach K, Martin A, Rizzo M, Kaiser R et al. Nintedanib plus docetaxel as second-line therapy in patients with non-small-cell lung cancer, a network meta-analysis. *Future Oncol* 2015, **11**(3), 409–420

32. Isomoto H, Kobayashi S, Werneburg NW, Bronk SF, Guicciardi ME, Frank DA et al. Interleukin 6 upregulates myeloid cell leukemia-1 expression through a STAT3 pathway in cholangiocarcinoma cells. *Hepatology* 2005, **42**(6), 1329–1338

33. Yu H, Lee H, Herrmann A, Buettner R, Jove R. Revisiting STAT3 signalling in

cancer, new and unexpected biological functions. *Nat Rev Cancer* 2014, **14**(11), 736–746

34. Zheng T, Hong X, Wang J, Pei T, Liang Y, Yin D et al. Gankyrin promotes tumor growth and metastasis through activation of IL-6/STAT3 signaling in human cholangiocarcinoma. *Hepatology* 2014, **59**(3), 935–946

35. Frampton G, Invernizzi P, Bernuzzi F, Pae HY, Quinn M, Horvat D et al. Interleukin-6-driven progranulin expression increases cholangiocarcinoma growth by an Akt-dependent mechanism. *Gut* 2012, **61**(2), 268–277

36. Lai Y, Liu XH, Zeng Y, Zhang Y, Shen Y, Liu Y. Interleukin-8 induces the endothelial cell migration through the Rac 1/RhoA-p38MAPK pathway. *Eur Rev Med Pharmacol Sci* 2012, **16**(5), 630–638

37. Palena C, Hamilton DH, RI Fernando. Influence of IL-8 on the epithelial-mesenchymal transition and the tumor microenvironment. *Future Oncol* 2012, **8**(6), 713–722

38. Lu X, Mu E, Wei Y, Riethdorf S, Yang Q, Yuan M et al. VCAM-1 promotes osteolytic expansion of indolent bone micrometastasis of breast cancer by engaging alpha4beta1-positive osteoclast progenitors. *Cancer Cell* 2011, **20**(6), 701–714

39. Peng H, Zhang Q, Li J, Zhang N, Hua Y, Xu L et al. Apatinib inhibits VEGF

signaling and promotes apoptosis in intrahepatic cholangiocarcinoma. *Oncotarget* 2016, **7**(13), 17220–17229

40. Chatterjee S, Heukamp LC, Siobal M, Schöttle J, Wieczorek C, Peifer M et al. Tumor VEGF, VEGFR2 autocrine feed-forward loop triggers angiogenesis in lung cancer. *J Clin Invest* 2013, **123**(4), 1732–1740

41. Sulpice L, Rayar M, Desille M, Turlin B, Fautrel A, Boucher E et al. Molecular profiling of stroma identifies osteopontin as an independent predictor of poor prognosis in intrahepatic cholangiocarcinoma. *Hepatology* 2013, **58**(6), 1992–2000

42. Zheng Y, Zhou C, Yu XX, Wu C, Jia HL, Gao XM et al. Osteopontin promotes metastasis of intrahepatic cholangiocarcinoma through recruiting MAPK1 and mediating Ser675 phosphorylation of beta-Catenin. *Cell Death Dis* 2018, **9**(2), 179

43. Guo Y, Xu F, Lu T, Duan Z, Zhang Z. Interleukin-6 signaling pathway in targeted therapy for cancer. *Cancer Treat Rev* 2012, **38**(7), 904–910

44. Sun L, Wang Q, Chen B, Zhao Y, Shen B, Wang H et al. Gastric cancer mesenchymal stem cells derived IL-8 induces PD-L1 expression in gastric cancer cells via STAT3/mTOR-c-Myc signal axis. *Cell Death Dis* 2018, **9**(9), 928

45. Zhao D, Pan C, Sun J, Gilbert C, Drews-Elger K, Azzam DJ et al. VEGF drives cancer-initiating stem cells through VEGFR-2/Stat3 signaling to upregulate Myc and

Sox2. Oncogene 2015, **34**(24), 3107–3119

46. Huyen NT, Prachayasittikul V, Chan-On W. Anoikis-resistant cholangiocarcinoma cells display aggressive characteristics and increase STAT3 activation. *J Hepatobiliary Pancreat Sci* 2016, **23**(7), 397–405

47. Gong J, Muñoz AR, Pingali S, Payton-Stewart F, Chan DE, Freeman JW et al. Downregulation of STAT3/NF-kappaB potentiates gemcitabine activity in pancreatic cancer cells. *Mol Carcinog* 2017, **56**(2), 402–411

48. Wormann SM et al. Loss of P53 function activates JAK2-STAT3 signaling to promote pancreatic tumor growth, stroma modification, and gemcitabine resistance in mice and is associated with patient survival. *Gastroenterology* 2016, **151**(1), 180–193e12

Figure legends

Figure 1. Effects of CAF on ICC cells *in vitro* and *in vivo*

(A) CM from CAF1 and CAF2 enhance the proliferation of both HuCCT1 and RBE (n = 5). *P < 0.01.

(B) CM from CAF1 and CAF2 enhance the invasive ability of both HuCCT1 and RBE (n = 5). *P < 0.01.

(C) The tumor growth curve of HuCCT1 and HuCCT1 plus CAF cells. The tumor growth of HuCCT1 + CAFs was much greater compared with that of HuCCT1 alone (n = 5). *P < 0.05.

Figure 2. Effects of nintedanib on CAFs and ICC cells

(A) Nintedanib inhibits the proliferation of CAF concentration-dependently (n = 5). *P < 0.01.

(B) Nintedanib inhibits the proliferation of HuCCT1and RBE only at high concentrations (n = 5). *P < 0.01.

(C) α-SMA expression in CAFs treated by nintedanib is evaluated by western blotting. CAFs pre-activated with 5 ng ml-1 TGF-b1. β-actin is used as the loading control. *P < 0.01.

Figure 3. Nintedanib inhibits the ICC promoting effects of CAFs.

(A) The proliferation-enhancing effects of CAF-CM on HuCCT1 and RBE are eliminated by nintedanib treatment (n = 5). *P < 0.01.

(B) The invasiveness enhancing effects of CAF-CM on HuCCT1 and RBE are decreased by nintedanib treatment (n = 5). *P < 0.01.

Figure 4. Nintedanib suppresses the cytokines secretion of CAFs

(A) Cytokine array comparing CAF-CM and nintedanib-treated CAF-CM. IL-6, IL-8, VEGF, VCAM1, and osteopontin were reduced by nintedanib treatment. The right panel shows the density ratio of array dots between CAF-CM and nintedanib-treated CAF-CM. Cytokine array was performed using CAF1.

(B) ELISA of IL-6 and IL-8 in CAF-CM and nintedanib-treated CAF-CM. IL-6 and IL-8 were reduced by nintedanib treatment (n = 5). *P < 0.01.

(C) The effects of CAF-CM and nintedanib-treated CAF-CM on the phosphorylation of STAT3 in HuCCT1 and RBE cell lines were evaluated by Western blotting. CAF-CM increased the phosphorylation of STAT3 in ICC cell lines, but the increasing effects were eliminated by nintedanib treatment.

Figure 5. Nintedanib reduces tumor volume consisting of HuCCT1 plus CAFs, and combination therapy with gemcitabine inhibits tumor proliferation markedly

(A) Tumor growth curve shows that combination therapy with nintedanib plus gemcitabine suppresses the growth of tumors consisting of HuCCT1 plus CAFs to the greatest extent. Photograph of tumors from the four treatment groups (control, nintedanib, gemcitabine, nintedanib + gemcitabine). GEM, gemcitabine (n = 6). *P < 0.05.

(B) Representative photomicrographs of histological examinations comparing the four treatment groups (control, nintedanib, gemcitabine, nintedanib + gemcitabine) (HE, α-SMA and Ki67, Original magnification ×200, scar bar 100 μm). Nintedanib treatment significantly reduced α-SMA-positive staining in stroma. Gemcitabine treatment significantly reduced the proportion of Ki-67-positive cells. Nintedanib plus gemcitabine treatment showed a reduction of both α-SMA-positive staining in stroma and the proportion of Ki-67 positive ICC cells. GEM, gemcitabine (n = 5). *P < 0.05.

Supplementary Figure 1. *In vivo* experimental schedule

(A) Comparison between HuCCT1 cells alone and HuCCT1 plus CAFs cells.

(B) Nintedanib and gemcitabine treatment schedule.

Supplementary Figure 2. Effects of CAF and nintedanib were observed in the supernatants of CM after ultracentrifugation

(A) The proliferation-enhancing effect and nintedanib treatment effect on HuCCT1 and RBE cell lines were observed only in the supernatants of CAF-CM and nintedanib-treated CAF-CM after ultracentrifugation.

Supplementary Figure 3. IL-6 and IL-8 promotes phosphorylation of STAT3 in ICC cells

(A) The effects of IL-6 and IL-8 on the phosphorylation of STAT3 in HuCCT1 were evaluated by Western blotting. IL-6 and IL-8 promoted the expression of the phospho-STAT3 in HuCCT1.

(B) With recombinant IL-6 and IL-8, the effects of nintedanib-treated CAF-CM on the proliferation and invasion of HuCCT1 were restored. ($n = 5$). *$P < 0.01$.

Supplementary Figure 4. Nintedanib treatment significantly reduced the number of phospho-STAT3 positive ICC cells

(A) The number of phospho-STAT3 in HuCCT1 was counted. Nintedanib treatment significantly reduced the number of pSTAT3 positive cells, with the greatest reduction observed with combined nintedanib and gemcitabine treatment. (n = 5). *P < 0.05.

Supplementary Figure 5. Body weight and serum biochemical tests of mice

(A) Relationship between mouse body weight and treatment group in the xenograft experiments. There was no correlation between the body weight and treatment group (n = 3).

(B) Effect of treatment on blood biochemical parameters. There was no apparent organ toxicity in each group. GEM, gemcitabine; ALT, alanine aminotransferase (n = 3).

Supplementary Figure 6. Effects of nintedanib on LX-2

Nintedanib also suppressed the proliferation and α-SMA expression of LX-2 (n = 5). *P < 0.01.

Figure 1

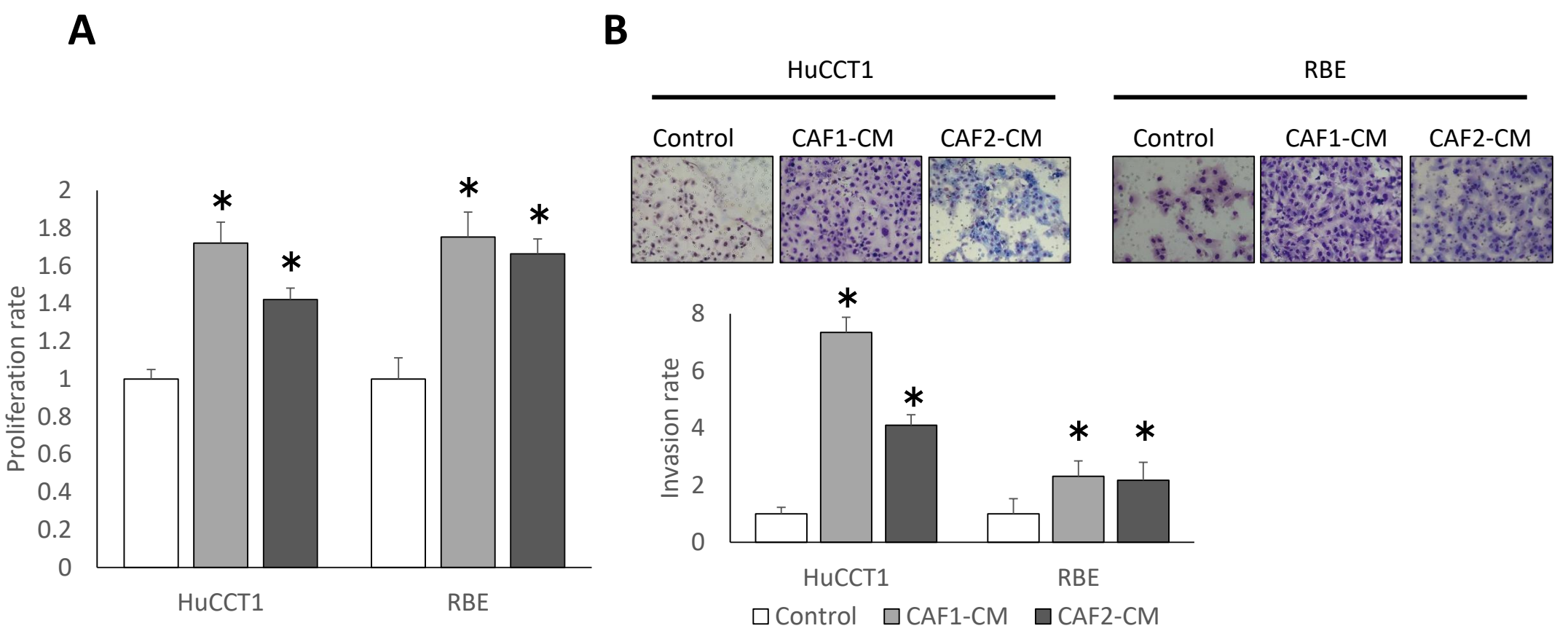
A
Proliferation rate
2
1.8
1.6
1.4
1.2
1
0.8
0.6
0.4
0.2
0
HuCCT1
RBE
Control
CAF1-CM
CAF2-CM
B
HuCCT1
RBE
Control
CAF1-CM
CAF2-CM
Control
CAF1-CM
CAF2-CM
Invasion rate
8
6
4
2
0
HuCCT1
RBE
Control
CAF1-CM
CAF2-CM

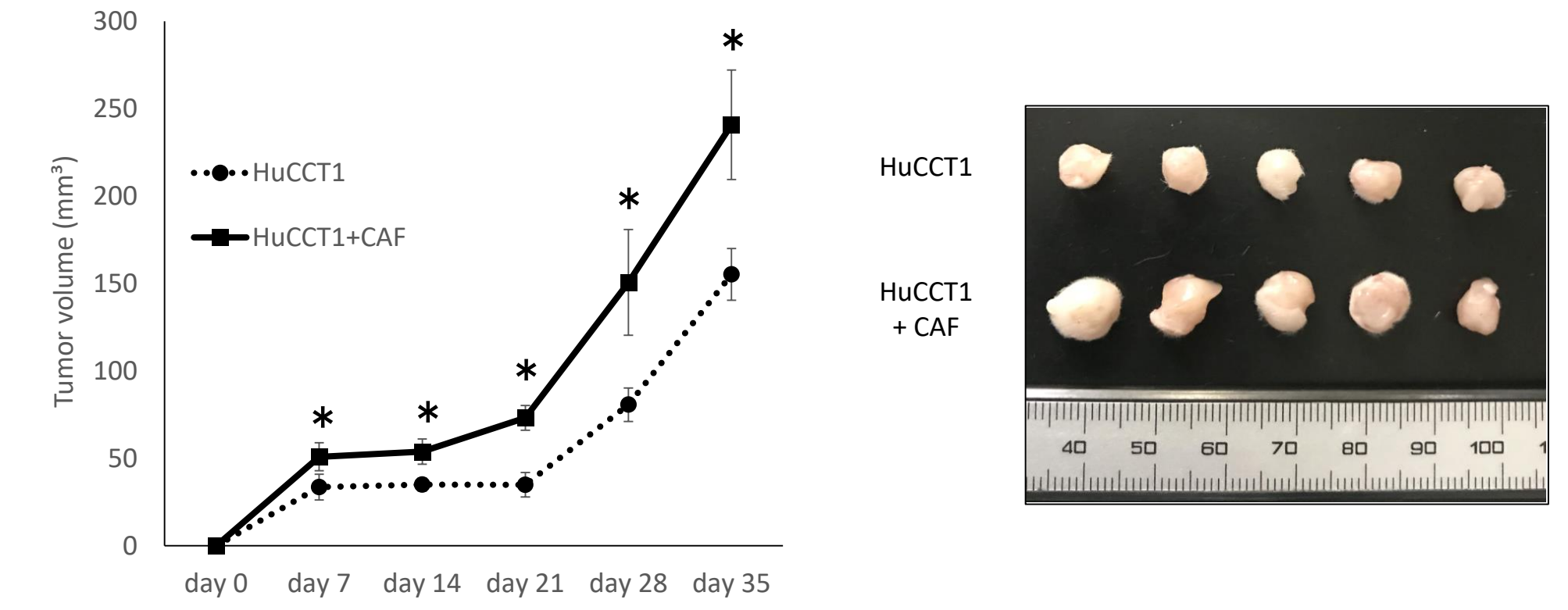
C
Tumor volume (mm³)
300
250
200
150
100
50
0
HuCCT1
HuCCT1+CAF
day 0
day 7
day 14
day 21
day 28
day 35
HuCCT1
HuCCT1
+ CAF
40
50
60
70
80
90
100

Figure 2

A

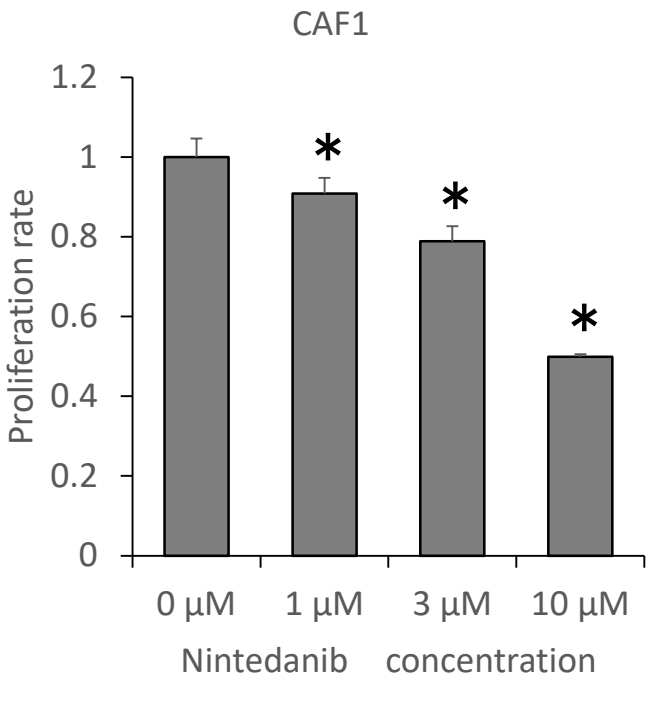
CAF1
Proliferation rate
1.2
1
0.8
0.6
0.4
0.2
0
*
*
*
0 μM
1 μM
3 μM
10 μM
Nintedanib concentration

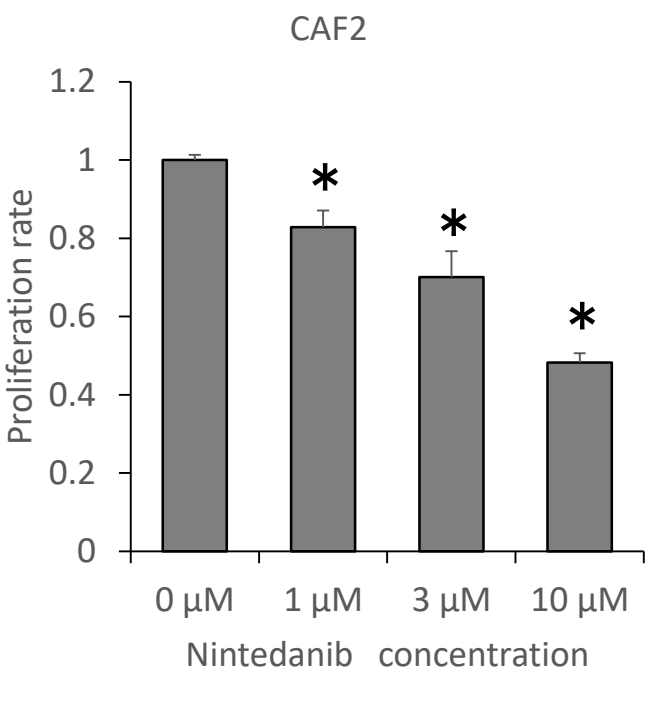
CAF2
Proliferation rate
1.2
1
0.8
0.6
0.4
0.2
0
*
*
*
0 μM
1 μM
3 μM
10 μM
Nintedanib concentration

B

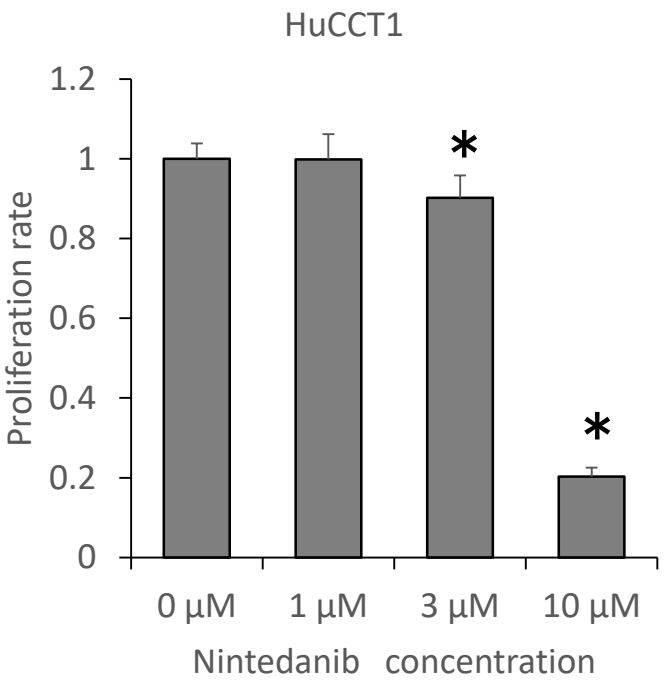
HuCCT1
Proliferation rate
1.2
1
0.8
0.6
0.4
0.2
0
*
*
0 μM
1 μM
3 μM
10 μM
Nintedanib concentration

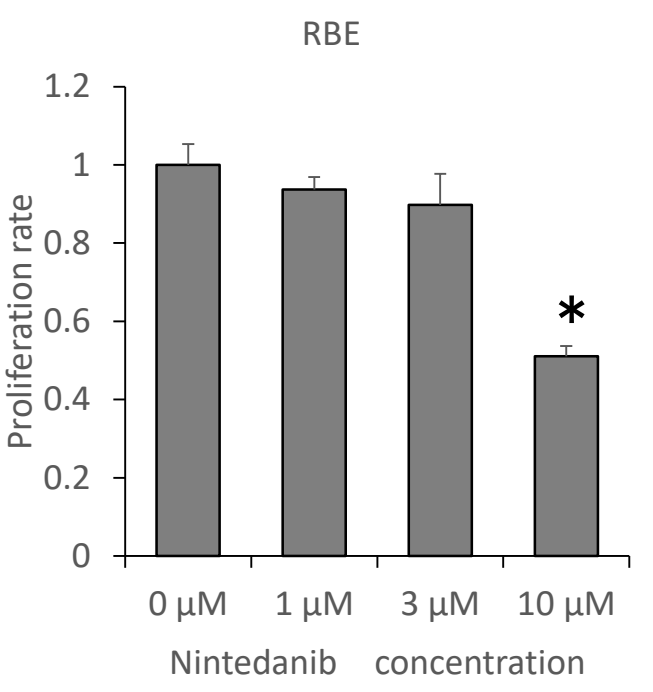
RBE
Proliferation rate
1.2
1
0.8
0.6
0.4
0.2
0
*
0 μM
1 μM
3 μM
10 μM
Nintedanib concentration

C

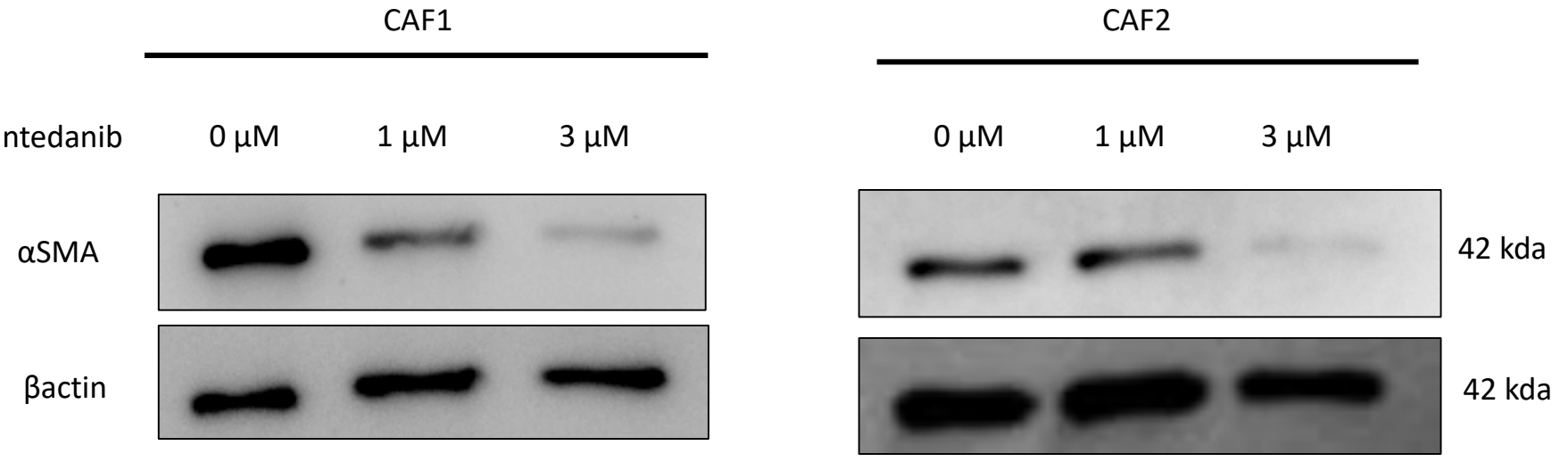
CAF1
CAF2
Nintedanib
0 μM
1 μM
3 μM
0 μM
1 μM
3 μM
αSMA
βactin
42 kda
42 kda

Figure 3

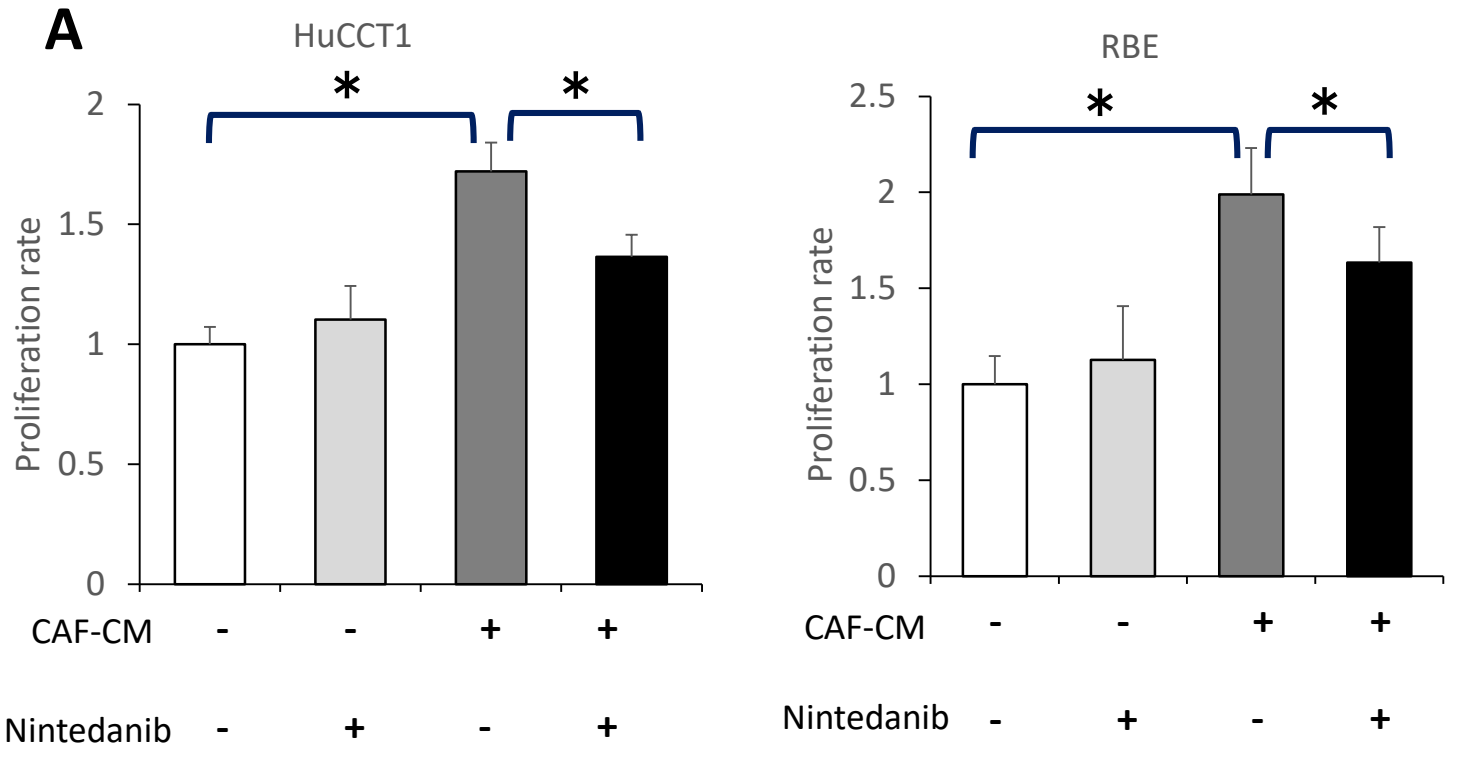
A
HuCCT1
RBE
Proliferation rate
2
1.5
1
0.5
0
2.5
*
*
CAF-CM - - + +
Nintedanib - + - +

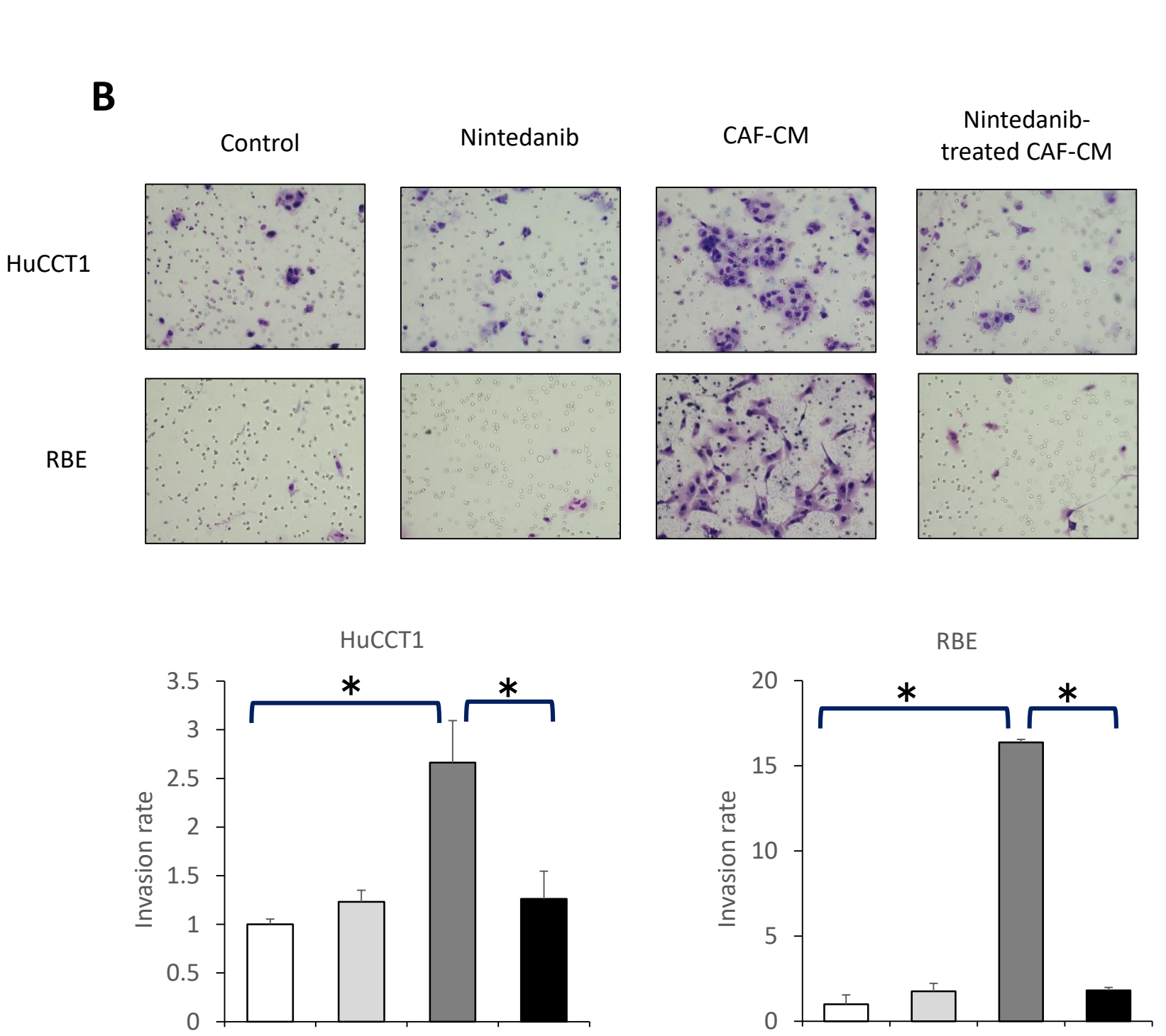
B
Control
Nintedanib
CAF-CM
Nintedanib-
treated CAF-CM
HuCCT1
RBE
HuCCT1
RBE
Invasion rate
3.5
3
2.5
2
1.5
1
0.5
0
20
15
10
5
0
*
*
CAF-CM - - + +
Nintedanib - + - +

Figure 4

A

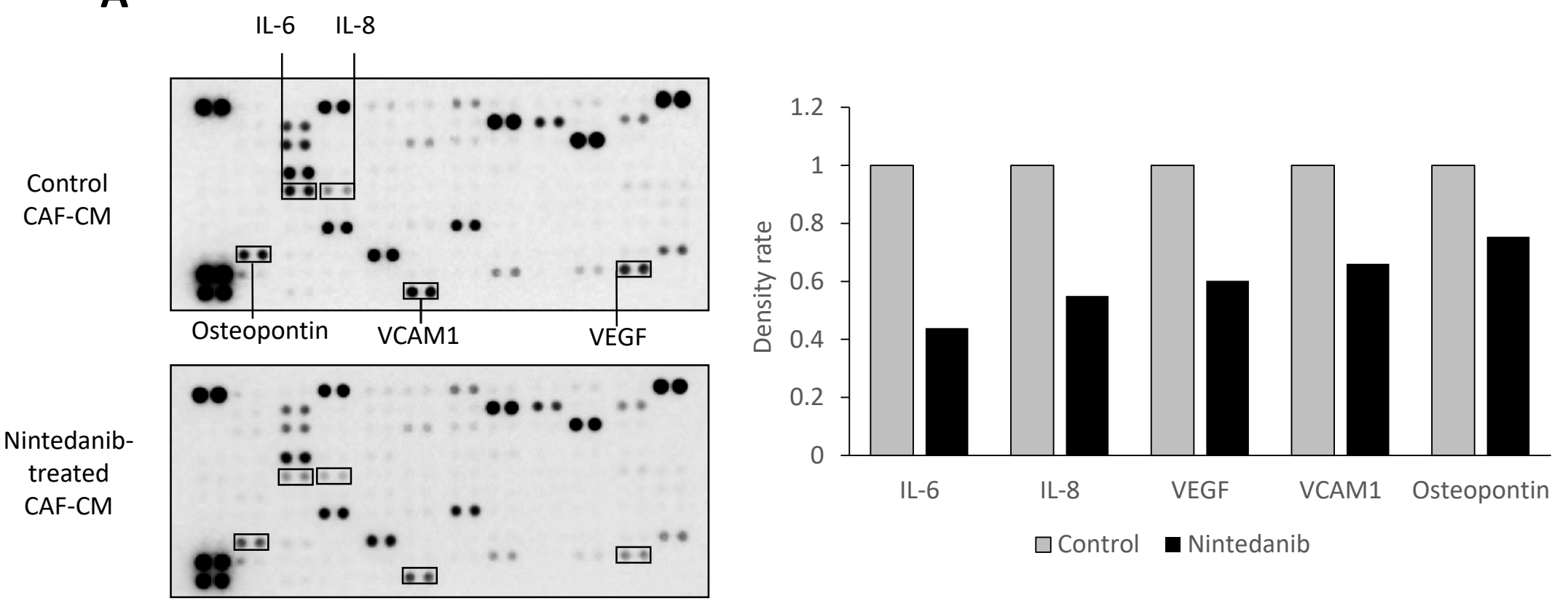
IL-6
IL-8
Control CAF-CM
Osteopontin
VCAM1
VEGF
Nintedanib-treated CAF-CM
Density rate
1.2
1
0.8
0.6
0.4
0.2
0
IL-6
IL-8
VEGF
VCAM1
Osteopontin
Control
Nintedanib

B

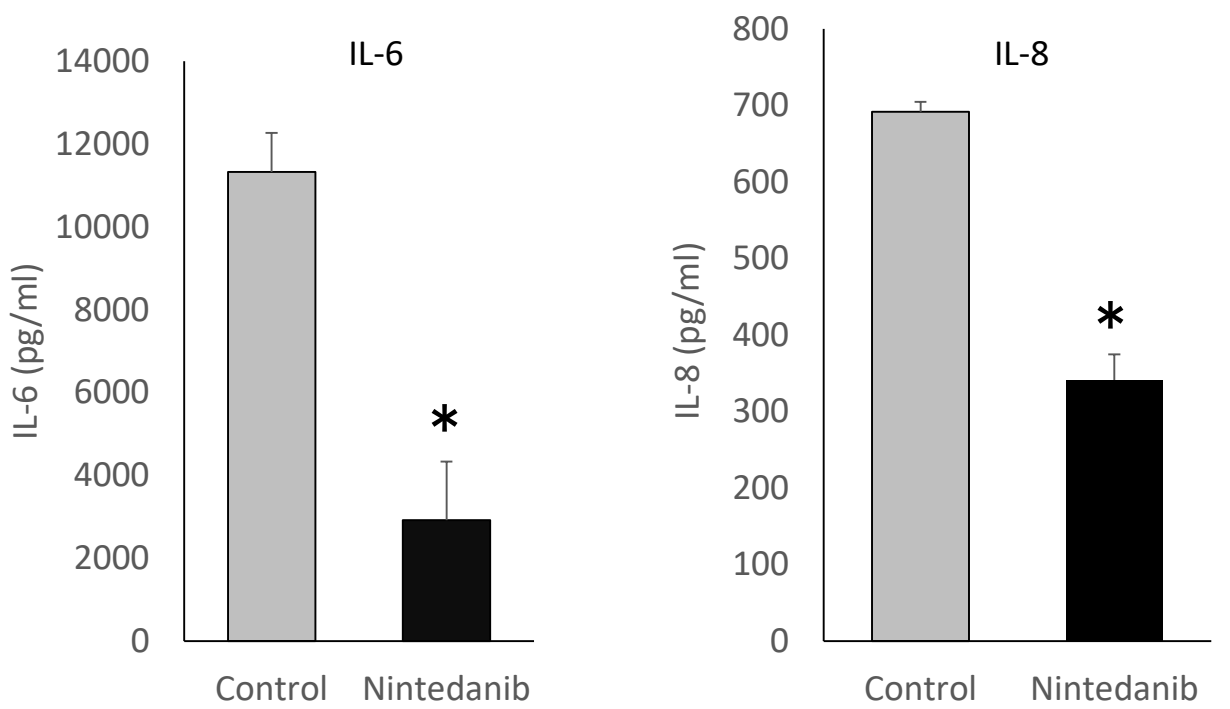
IL-6
IL-6 (pg/ml)
14000
12000
10000
8000
6000
4000
2000
0
*
Control
Nintedanib
IL-8
IL-8 (pg/ml)
800
700
600
500
400
300
200
100
0
*
Control
Nintedanib

C

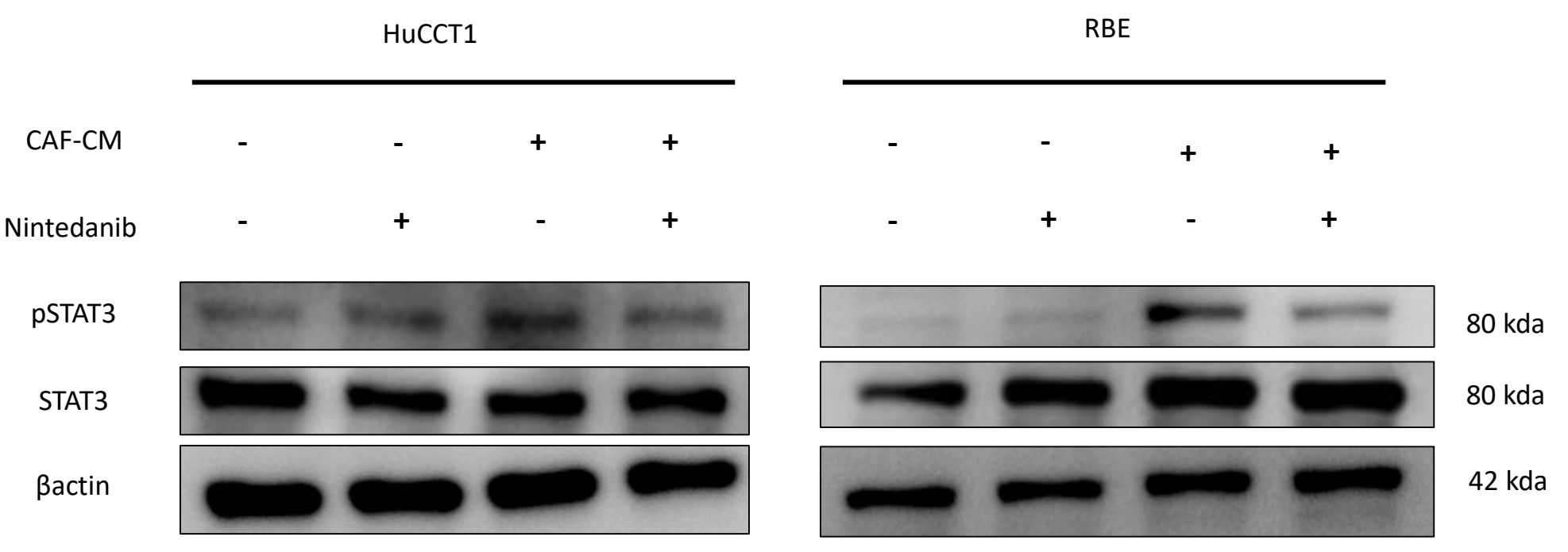
HuCCT1
RBE
CAF-CM
Nintedanib
pSTAT3
STAT3
βactin
80 kda
80 kda
42 kda

Figure 5

A

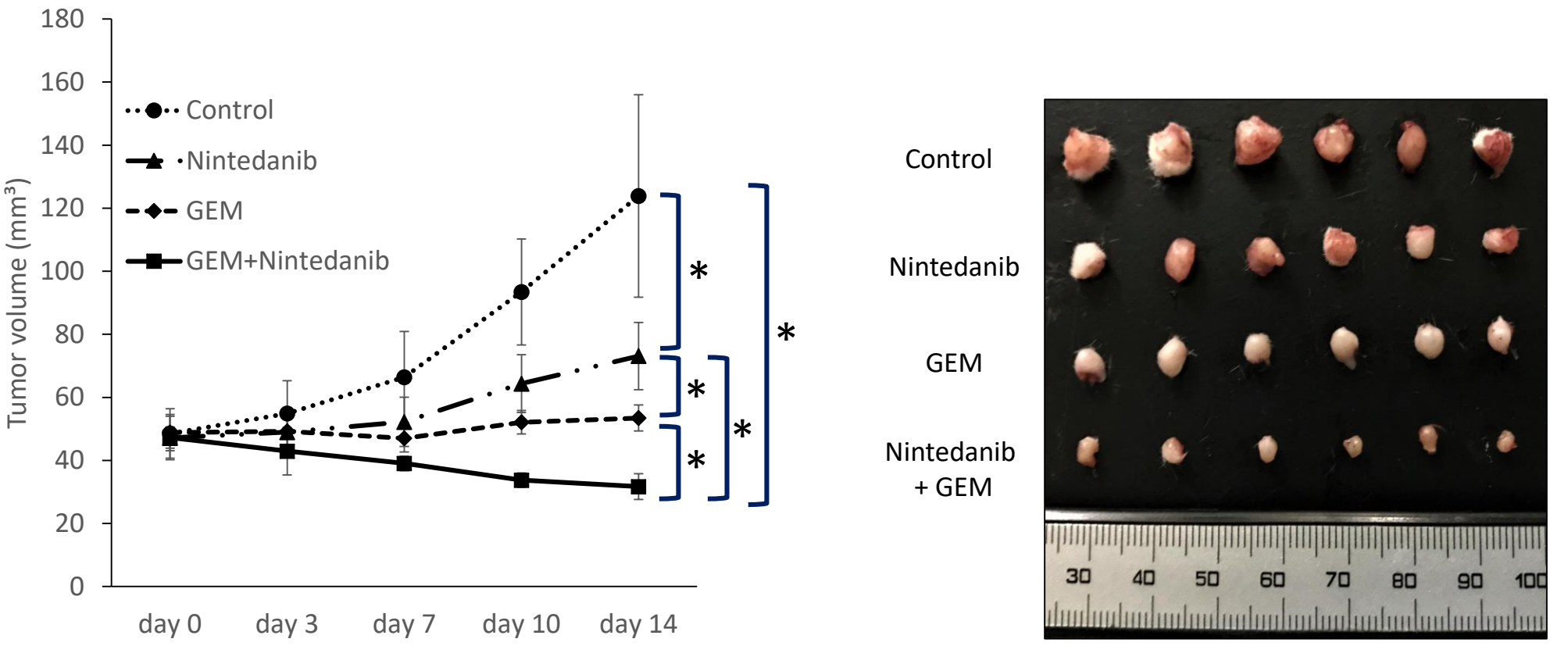
Tumor volume (mm³)
180
160
140
120
100
80
60
40
20
0
Control
Nintedanib
GEM
GEM+Nintedanib
*
*
*
*
day 0
day 3
day 7
day 10
day 14
Control
Nintedanib
GEM
Nintedanib + GEM
30
40
50
60
70
80
90
100

B

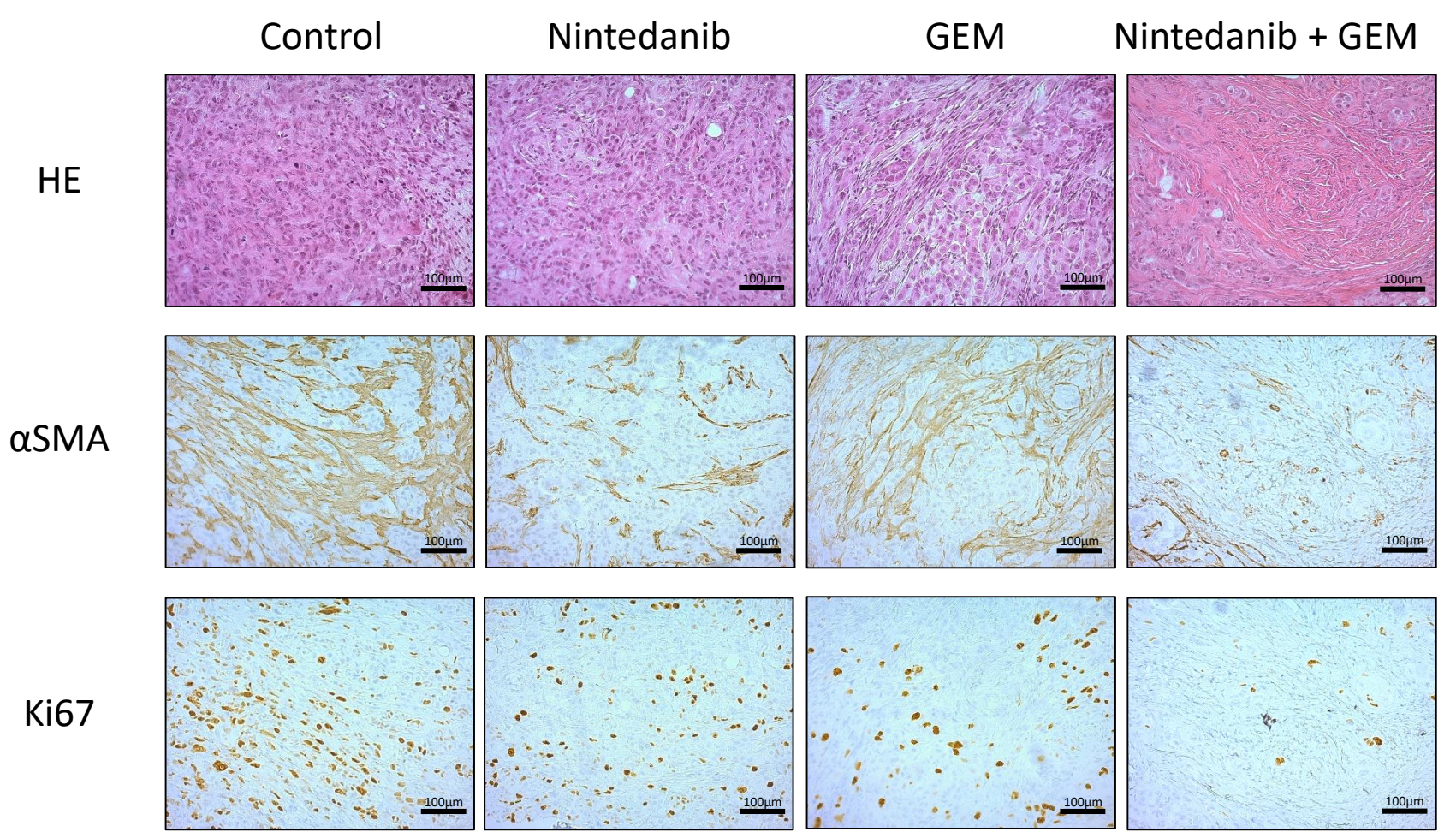
Control
Nintedanib
GEM
Nintedanib + GEM
HE
αSMA
Ki67
100μm

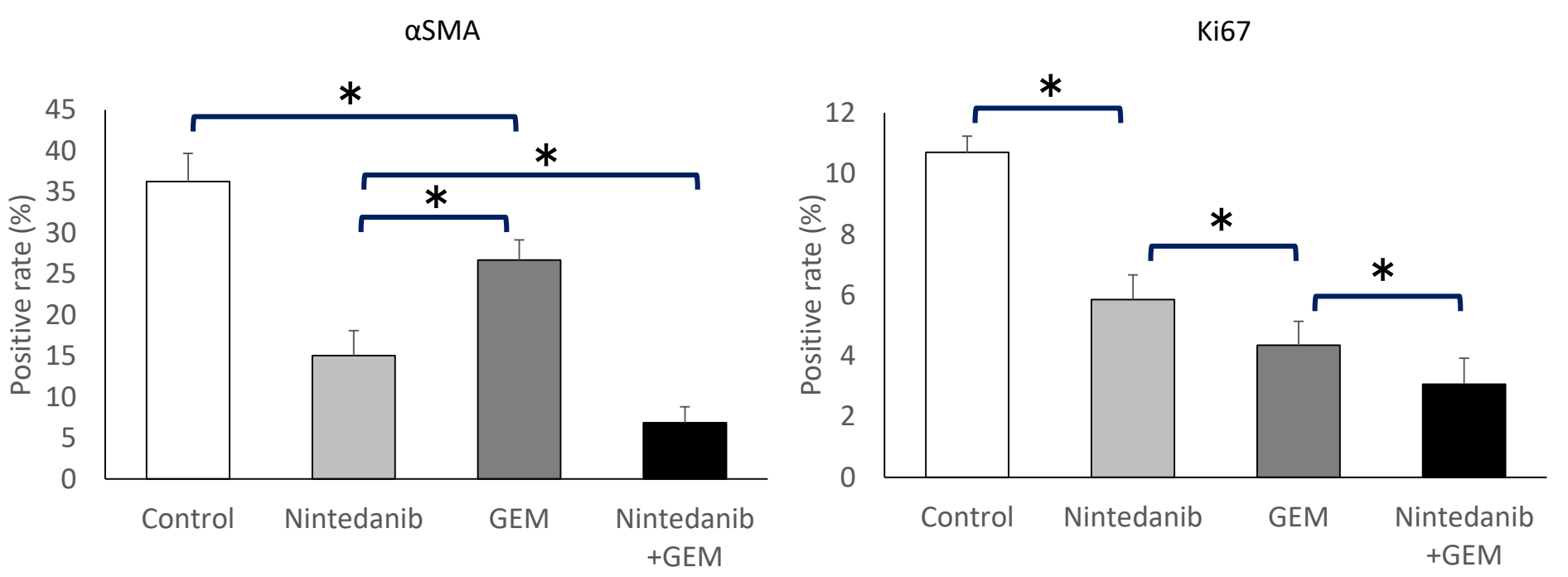
αSMA
Positive rate (%)
45
40
35
30
25
20
15
10
5
0
*
*
*
Control
Nintedanib
GEM
Nintedanib +GEM
Ki67
Positive rate (%)
12
10
8
6
4
2
0
*
*
*
Control
Nintedanib
GEM
Nintedanib +GEM

Figure 5

B

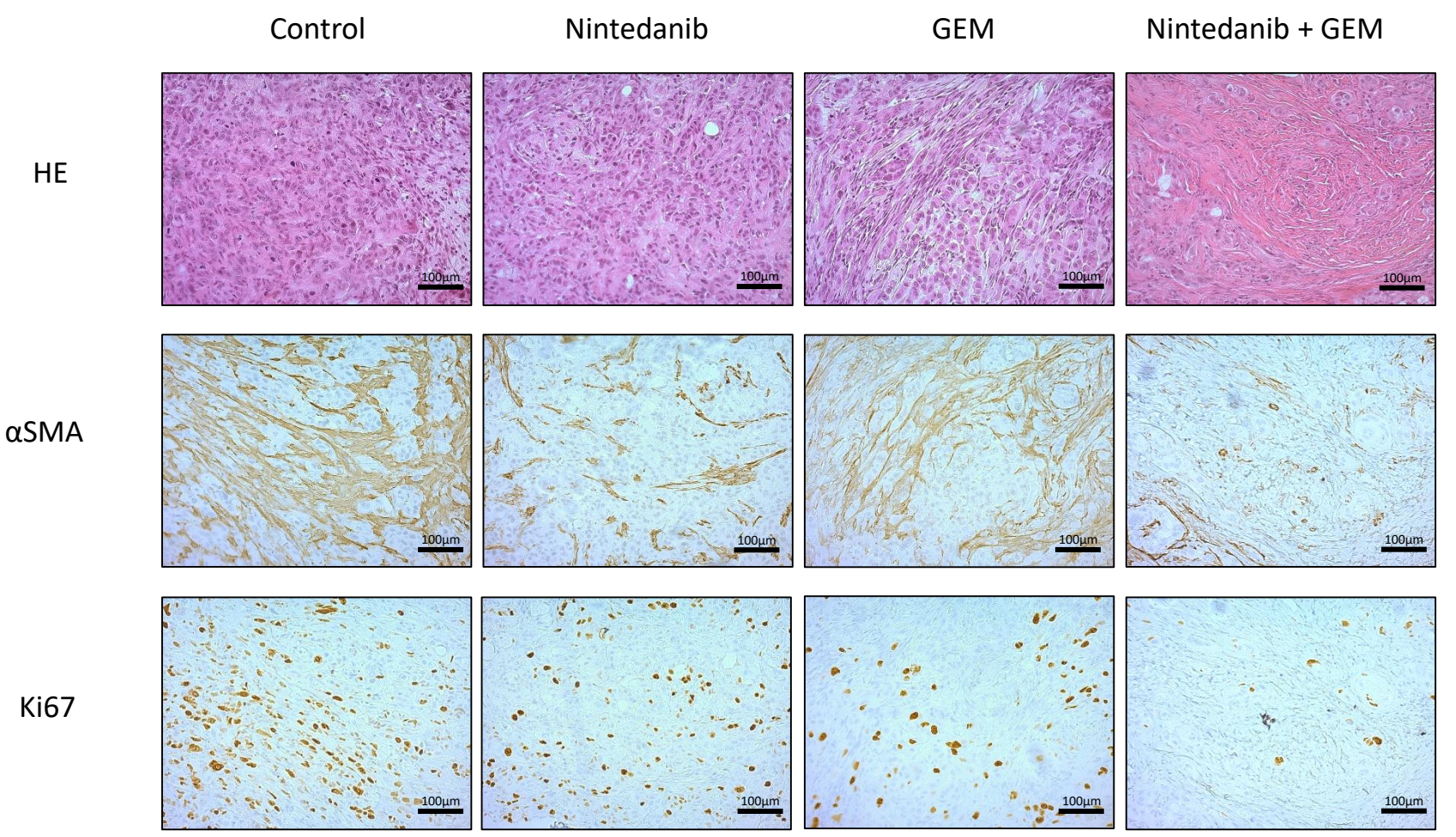

Supplementary Figure 1

A

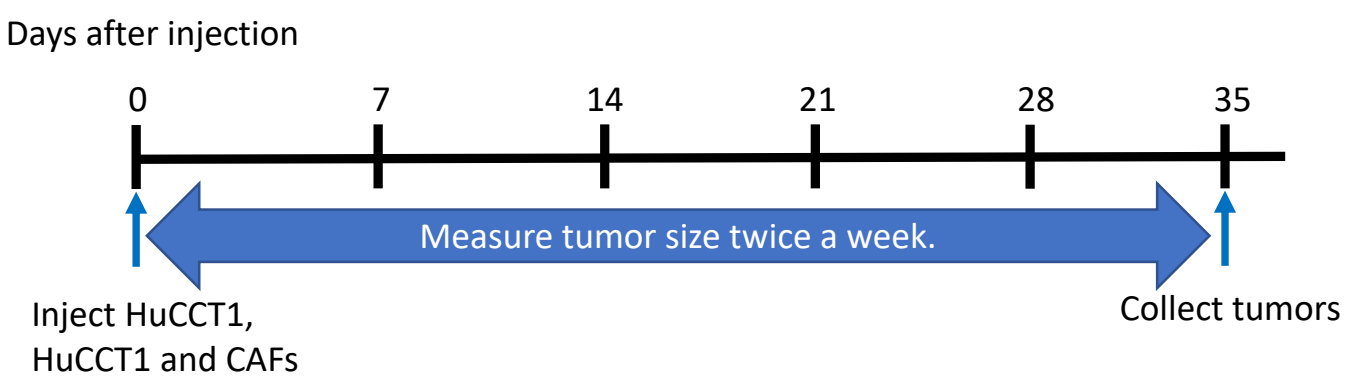

B

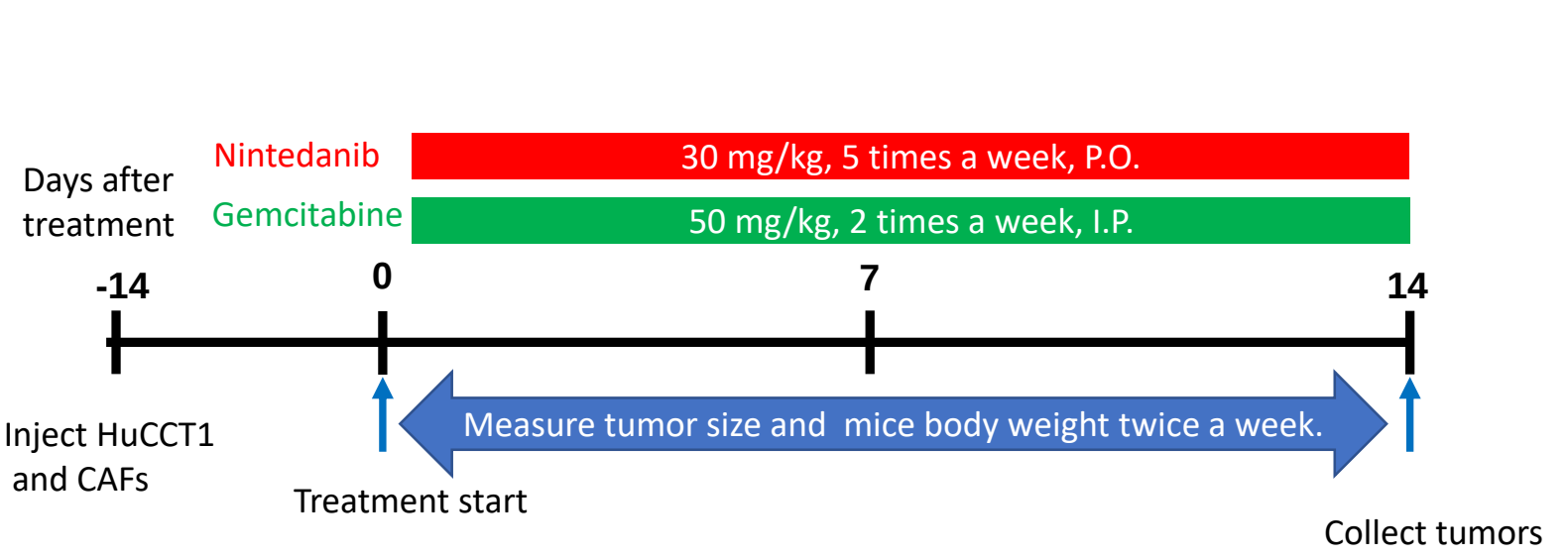

Supplementary Figure 2

A

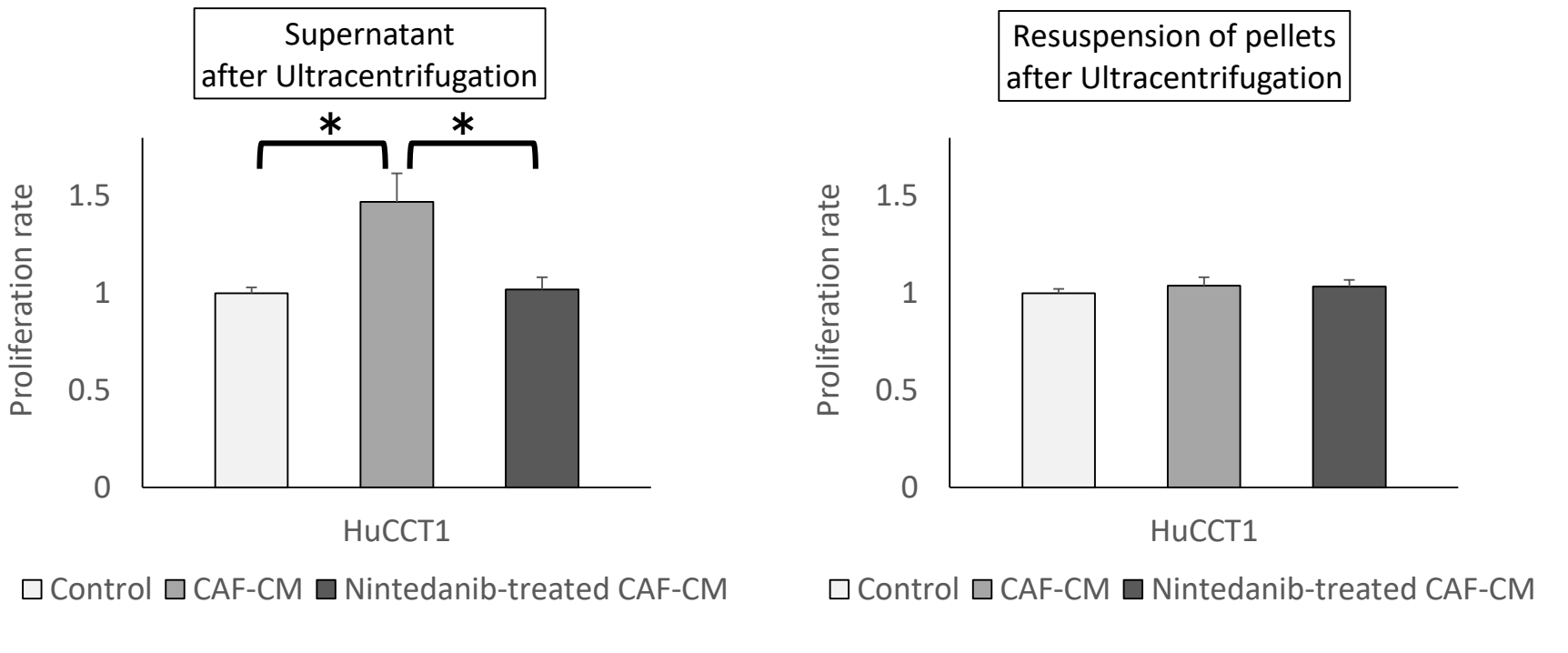

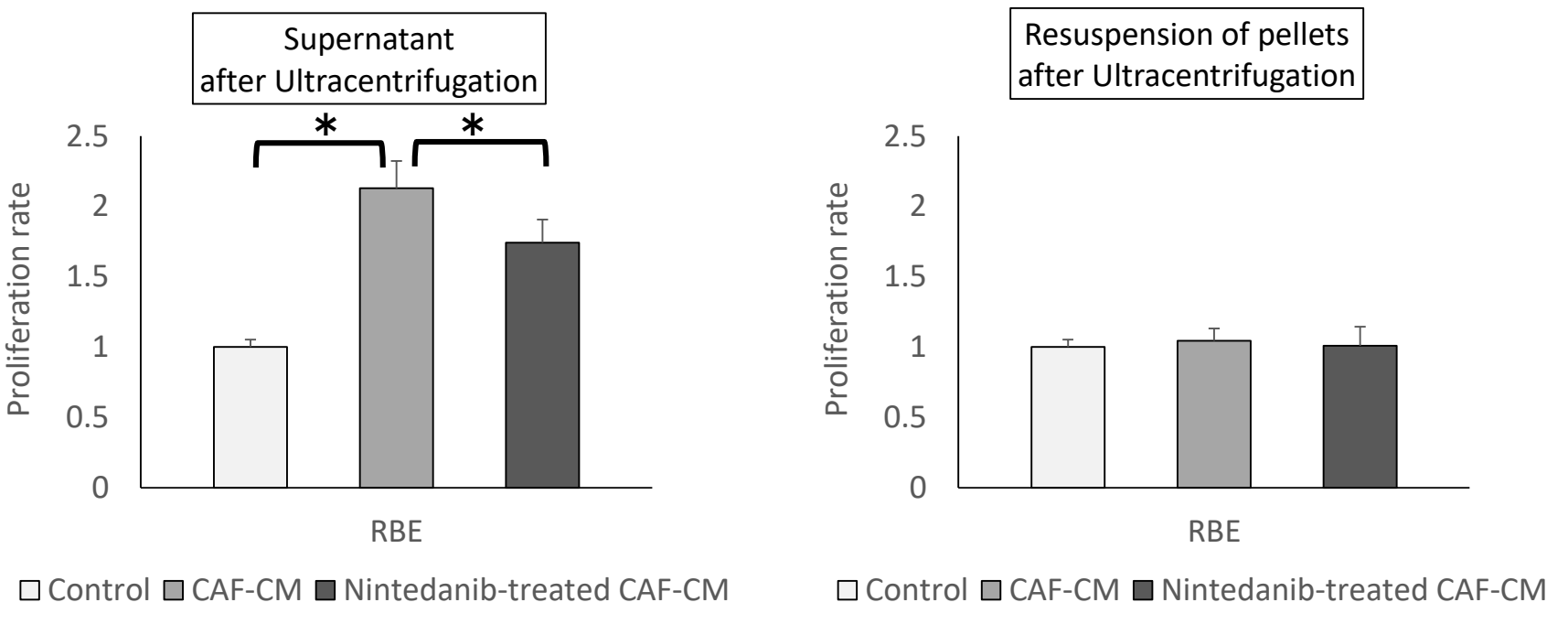

Supplementary Figure 3

A

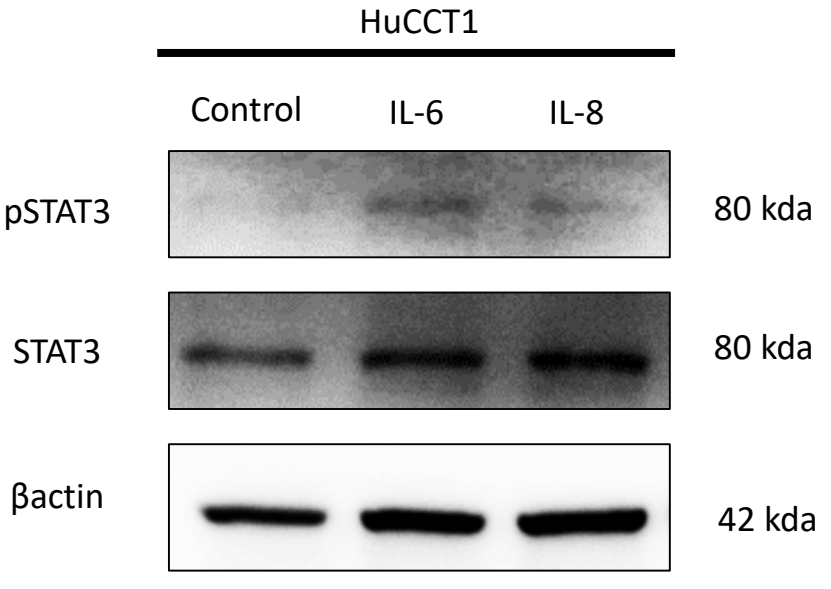

B

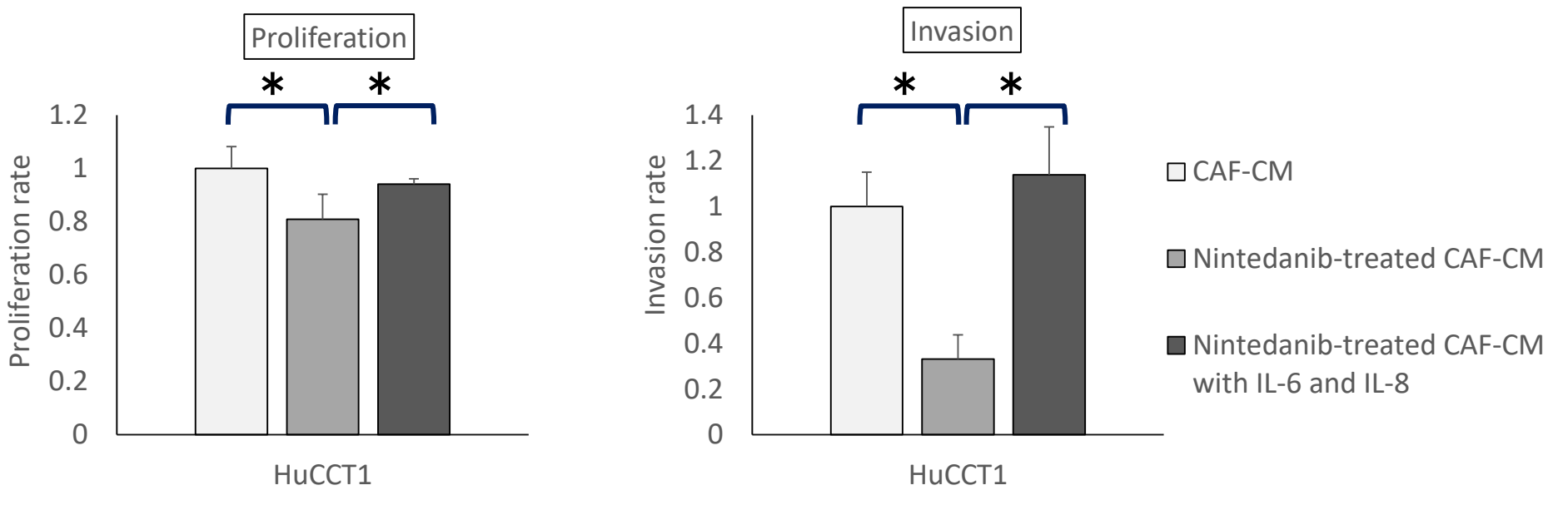

Supplementary Figure 4

A

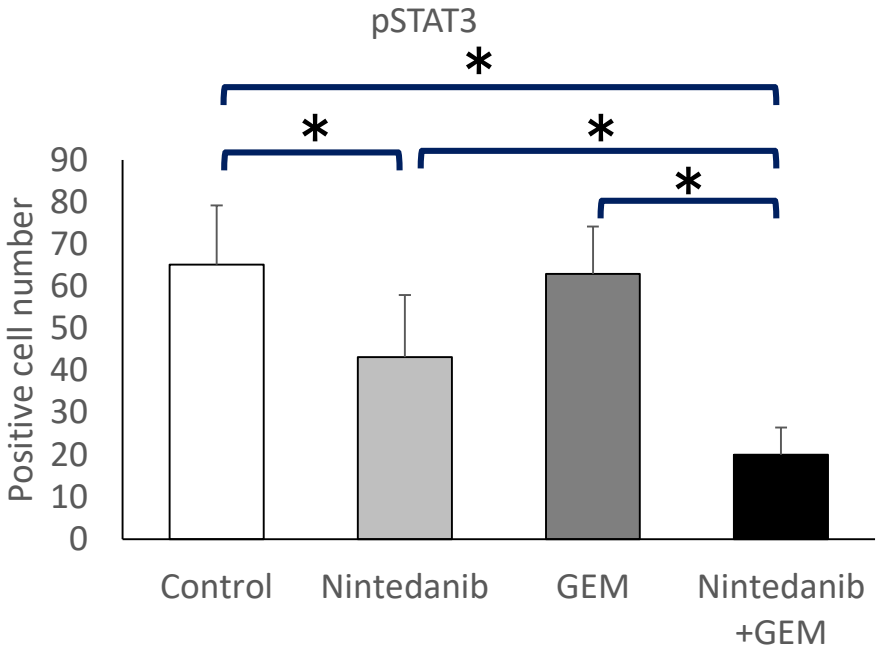

Supplementary Figure 5

A

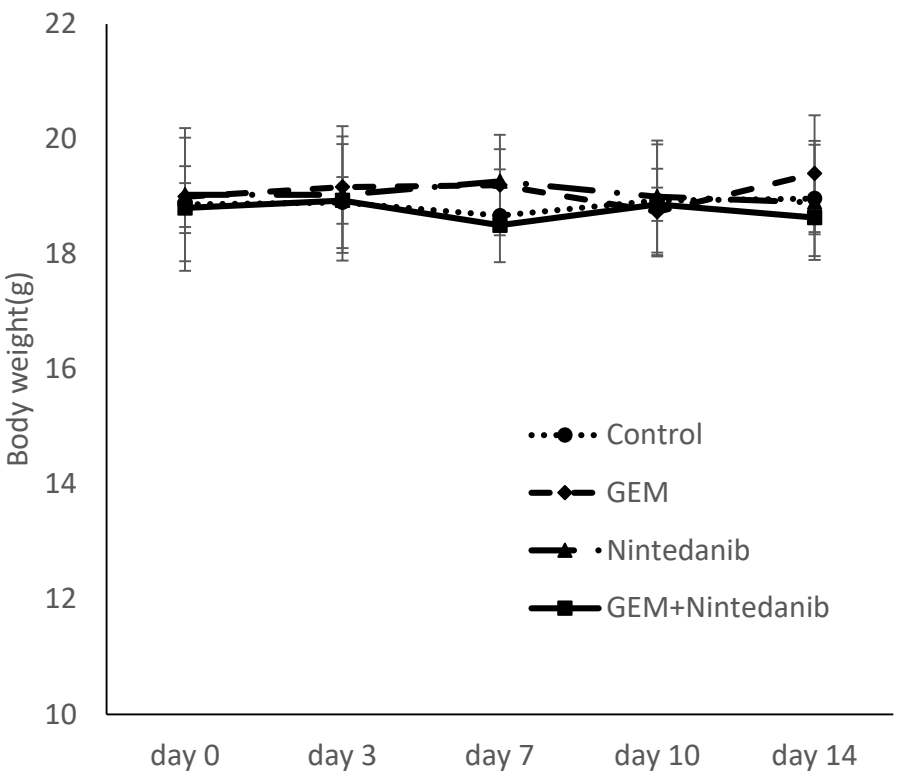

B

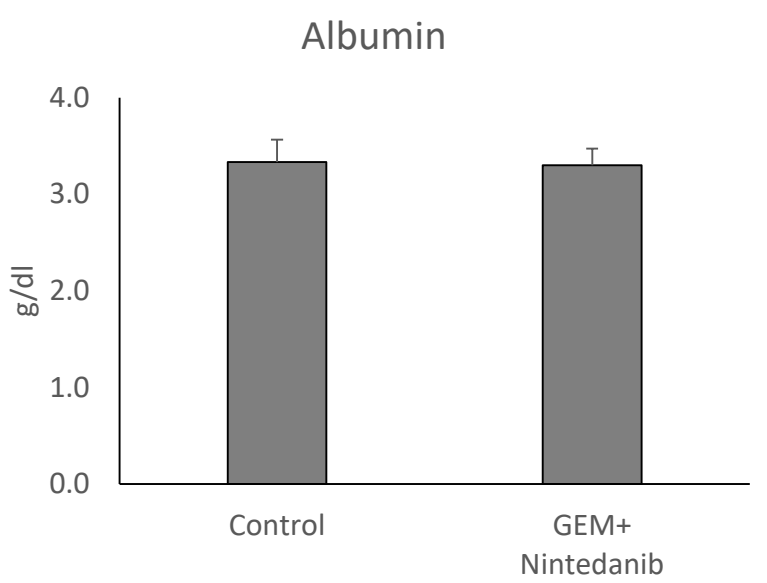

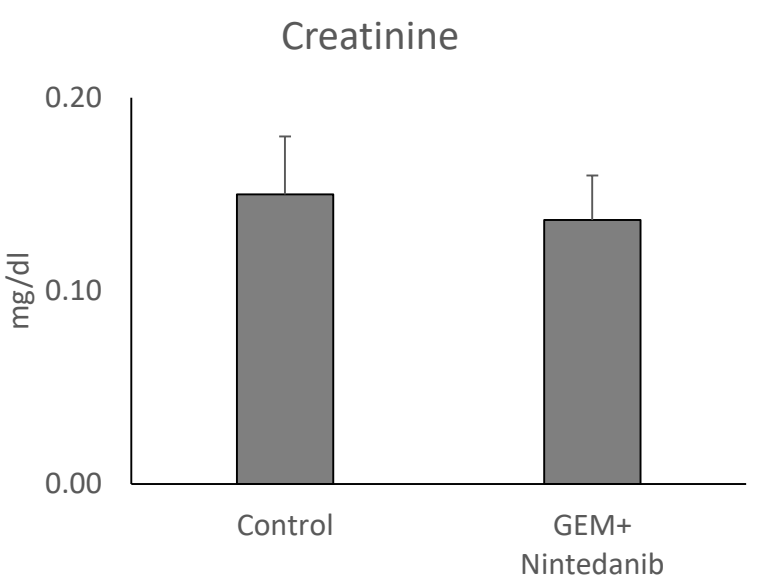

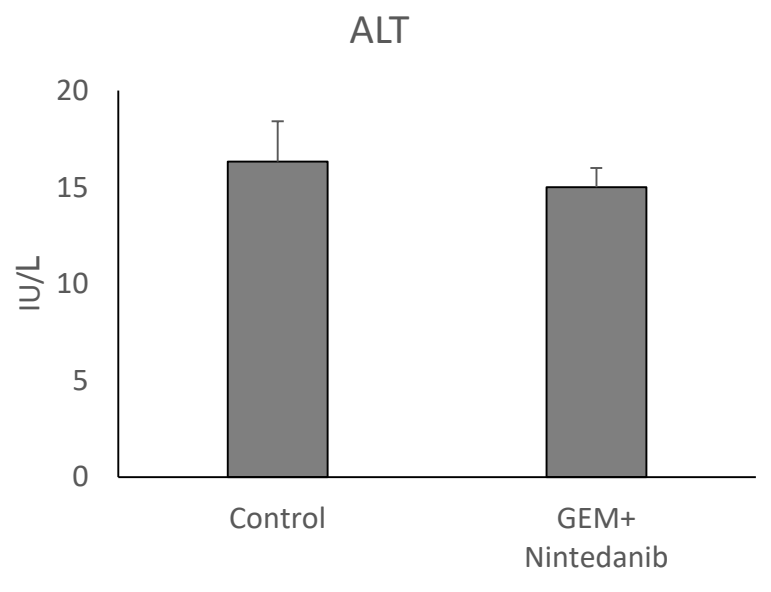

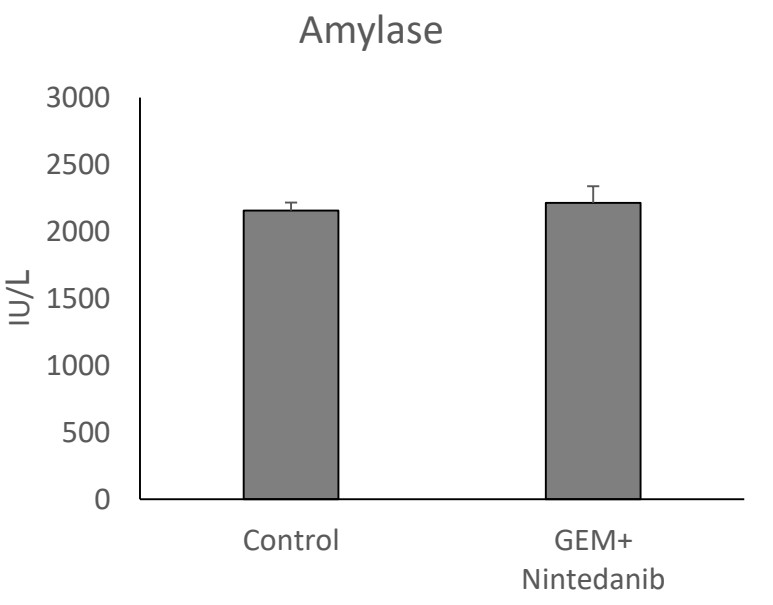

Supplementary Figure 6

A

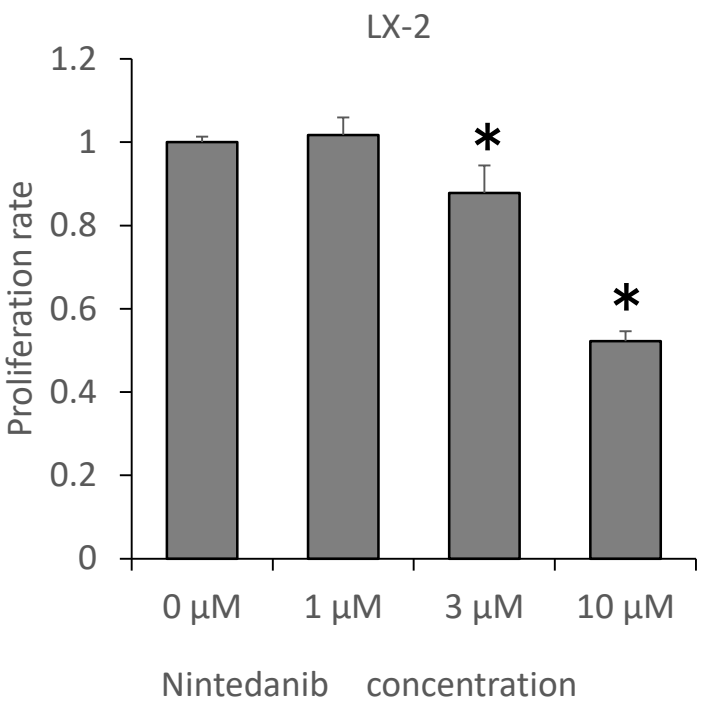

B

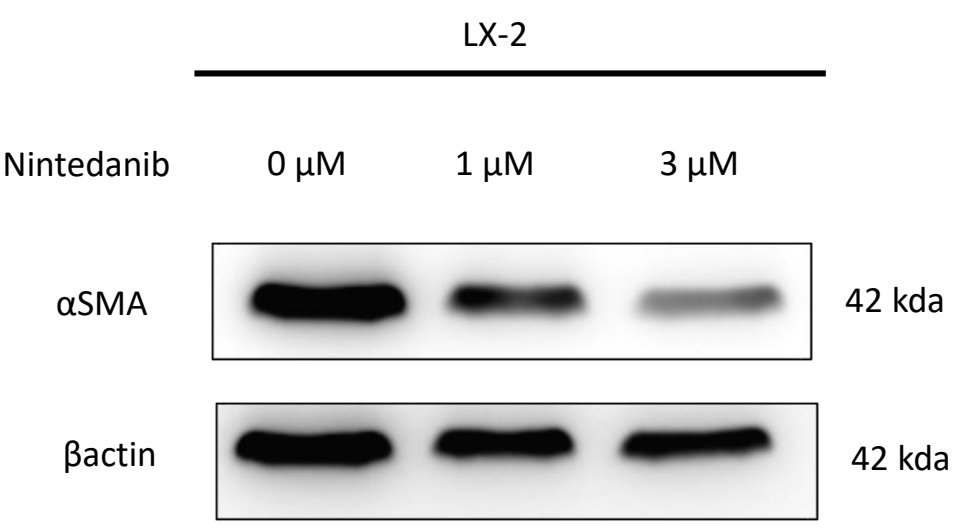

105 types of Cytokines and Proteins			
Interleukins	**Chemokines**	**Growth factors**	**Others**
IL-1 alpha/IL-1F1	CCL2/MCP-1	FGF basic	IFN-gamma
IL-1 beta/IL-1F2	CCL7/MCP-3	KGF/FGF-6	M-CSF
IL-1ra/IL-1F3	CXCL9/MIG	FGF-18	G-CSF
IL-2	CCL3/CCL4 MIP-1 alpha/beta	EGF	GM-CSF
IL-3	CCL20/MIP-3 alpha	HGF	TNF-alpha
IL-4	CCL19/MIP-3 beta	PDGF-AA	Leptin
IL-5	CXCL10/IP-10	PDGF-AB/BB	BAFF/BLyS/TNFSF13B
IL-6	CXCL11/I-TAC	VEGF	Adiponectin/Acrp30
IL-8	CXCL4/PF4	TGF-alpha	Angiogenin
IL-10	CCL5/RANTES		Angiopoietin-1
IL-11	CXCL12/SDF-1 alpha		Angiopoietin-2
IL-12 p70	CCL17/TARC		Apolipoprotein A1
IL-13	CXCL5/ENA-78		BDNF
IL-15	CXCL1/GRO alpha		CD14
IL-16			CD30
IL-17A			CD31/PECAM-1
IL-18 BPa			CD40 Ligand/TNFSF5
IL-19			Chitinase 3-like
IL-22			Complement Component C5/C5a
IL-23			Complement Factor D
IL-24			C-Reactive Protein/CRP
IL-27			Cripto-1
IL-31			Cystatin C
IL-32 alpha/beta/gamma			Dkk-1
IL-33			DPPIV/CD26
IL-34			Endoglin/CD105
			EMMPRIN
			Fas Ligand
			Flt-3 Ligand
			GDF-15
			Growth Hormone (GH)
			ICAM-1/CD54
			IGFBP-2
			IGFBP-3
			Kallikrein 3/PSA
			LIF
			Lipocalin-2/NGAL
			MIF
			MMP-9
			Myeloperoxidase
			Osteopontin (OPN)
			Pentraxin 3/TSF-14
			RAGE
			RBP4
			Relaxin-2
			Resistin
			Serpin E1/PAI-1
			SHBG
			ST2/IL1 R4
			TFF3
			TfR
			Thrombospondin-1
			TIM-1
			uPAR
			VCAM-1
			Vitamin D BP